

Ionization photophysics and spectroscopy of cyanoacetylene

Sydney Leach, Gustavo A. Garcia, Ahmed Mahjoub, Yves Bénilan, Nicolas Fray, Marie-Claire Gazeau, François Gaie-Levrel, Norbert Champion, and Martin Schwell

Citation: *The Journal of Chemical Physics* **140**, 174305 (2014); doi: 10.1063/1.4871298

View online: <http://dx.doi.org/10.1063/1.4871298>

View Table of Contents: <http://scitation.aip.org/content/aip/journal/jcp/140/17?ver=pdfcov>

Published by the [AIP Publishing](#)

Articles you may be interested in

[Ionization photophysics and spectroscopy of dicyanoacetylene](#)

J. Chem. Phys. **139**, 184304 (2013); 10.1063/1.4826467

[A femtosecond velocity map imaging study on B-band predissociation in CH₃I. II. The 2 0 1 and 3 0 1 vibronic levels](#)

J. Chem. Phys. **136**, 074303 (2012); 10.1063/1.3683252

[Resonantly enhanced multiphoton ionization and zero kinetic energy photoelectron spectroscopy of 2-indanol conformers](#)

J. Chem. Phys. **124**, 204306 (2006); 10.1063/1.2201747

[Resonantly enhanced two photon ionization and zero kinetic energy spectroscopy of jet-cooled 4-aminopyridine](#)

J. Chem. Phys. **120**, 7497 (2004); 10.1063/1.1687673

[Multiphoton ionization and photoelectron spectroscopy of formaldehyde via its 3p Rydberg states](#)

J. Chem. Phys. **114**, 9797 (2001); 10.1063/1.1370943



Re-register for Table of Content Alerts

Create a profile.



Sign up today!



Ionization photophysics and spectroscopy of cyanoacetylene

Sydney Leach,^{1,a)} Gustavo A. Garcia,² Ahmed Mahjoub,³ Yves Bénilan,³ Nicolas Fray,² Marie-Claire Gazeau,³ François Gaie-Levrel,^{2,b)} Norbert Champion,¹ and Martin Schwell^{3,a)}

¹LERMA UMR CNRS 8112, Observatoire de Paris-Meudon, 5 place Jules-Jansen, 92195 Meudon, France

²Synchrotron SOLEIL, L'Orme des Merisiers, St. Aubin, B.P. 48, 91192, Gif-sur-Yvette Cedex, France

³LISA UMR CNRS 7583, Université Paris Est Créteil and Université Paris Diderot, Institut Pierre Simon Laplace, 61 Avenue du Général de Gaulle, 94010 Créteil, France

(Received 26 January 2014; accepted 2 April 2014; published online 7 May 2014)

Photoionization of cyanoacetylene was studied using synchrotron radiation over the non-dissociative ionization excitation range 11–15.6 eV, with photoelectron-photoion coincidence techniques. The absolute ionization cross-section and spectroscopic aspects of the parent ion were recorded. The adiabatic ionization energy of cyanoacetylene was measured as 11.573 ± 0.010 eV. A detailed analysis of photoelectron spectra of HC_3N involves new aspects and new assignments of the vibrational components to excitation of the $\text{A}^2\Sigma^+$ and $\text{B}^2\Pi$ states of the cation. Some of the structured autoionization features observed in the 11.94 to 15.5 eV region of the total ion yield (TIY) spectrum were assigned to two Rydberg series converging to the $\text{B}^2\Pi$ state of HC_3N^+ . A number of the measured TIY features are suggested to be vibrational components of Rydberg series converging to the $\text{C}^2\Sigma^+$ state of HC_3N^+ at ≈ 17.6 eV and others to valence shell transitions of cyanoacetylene in the 11.6–15 eV region. The results of quantum chemical calculations of the cation electronic state geometries, vibrational frequencies and energies, as well as of the C–H dissociation potential energy profiles of the ground and electronic excited states of the ion, are compared with experimental observations. Ionization quantum yields are evaluated and discussed and the problem of adequate calibration of photoionization cross-sections is raised.

© 2014 AIP Publishing LLC. [<http://dx.doi.org/10.1063/1.4871298>]

I. INTRODUCTION

Cyanoacetylene, HC_3N , synthesized since the early 1900s,¹ is a useful reagent in cycloaddition reactions and in the synthesis of organometallic compounds, as an intermediate in pharmaceutical chemistry, and as an important reagent in laboratory studies of nucleobase assembly.² It possesses one CN triple bond and one CC triple bond. It is of interest to compare its chemical structure (Scheme 1(a)) with that of two related molecules, diacetylene, C_4H_2 , which has two conjugated CC triple bonds (Scheme 1(b)), and a central C–C single bond, and dicyanoacetylene, which has three conjugated triple bonds (Scheme 1(c)), the central bond being a $\text{C}\equiv\text{C}$ triple bond. Cyanoacetylene is thus apparently closer in structure to diacetylene, but the intercalation of nitrogen orbitals with those of carbon in creating molecular orbitals creates considerable differences.

The three molecules are linear. Diacetylene and dicyanoacetylene both possess a centre of symmetry (point group $D_{\infty h}$), which is lost in cyanoacetylene ($C_{\infty v}$), making the latter more complex in electronic transitions and general spectroscopy. We have previously studied aspects of the ionization photophysics and Rydberg spectroscopy of

diacetylene³ and dicyanoacetylene⁴ that are, like cyanoacetylene, molecules which have considerable astrophysical interest. The presence of a centre of symmetry in linear diacetylene and dicyanoacetylene prohibits observation of these molecules in the interstellar medium (ISM) by rotational microwave spectroscopy. This disadvantage does not exist for cyanoacetylene which has been observed in dark clouds^{5,6} in the ISM, including extragalactic sources,⁷ as well as in hot circumstellar environments such as the outflow of the carbon star IRC + 10216.⁸ Cyanoacetylene has also been observed in comets by radiofrequency spectroscopy, in comet Halle-Bopp⁹ and very recently (March 2013) in comet C/2012 F6 (Comet Lemmon).¹⁰ Models of the infra-red fluorescence of cyanoacetylene in cometary atmospheres have been developed.^{11,12}

One of the principal astrophysical interests of cyanoacetylene results from its observation by infrared spectroscopy in the stratosphere of Titan.^{13,14} The atmosphere of Titan consists mainly of N_2 gas. Nitrogen atoms formed by diverse dissociation processes react with other



SCHEME 1. Structure of cyanoacetylene (a), diacetylene (b), and dicyanoacetylene (c).

^{a)} Authors to whom correspondence should be addressed. Electronic addresses: Sydney.Leach@obspm.fr, Telephone: +33-1-4507-7561, Fax: +33-1-4507-7100 and Martin.Schwell@lisa.u-pec.fr, Telephone: +33-1-4517-1521, Fax: +33-1-4517-1564.

^{b)} Present address: Laboratoire national de métrologie et d'essais (LNE), 1 rue Gaston Boissier, 75724 Paris cedex 15, France.

ambient gases (e.g., methane) to synthesize a large number of hydrocarbons and nitriles.¹⁵ Complex nitrogen-bearing molecules are precursors for the production of the aerosol particles that are responsible for Titan's atmospheric haze.¹⁶

The atmosphere of Titan is the site of photochemical processes induced by various energy sources: solar irradiation, energetic particles existing in Saturn's magnetosphere and galactic cosmic rays. These are capable not only of initiating chemistry involving neutral species but also of inducing ionization processes.¹⁷ The photochemistry of cyanoacetylene is not only of considerable interest in the context of the atmosphere of Titan^{18–20} but also in aspects of origin of life studies where it is often considered as a key molecule or cation in formation processes of biological molecules.²¹ Laboratory studies of the photochemistry of cyanoacetylene have led to considerable understanding of the principal photodissociation processes.^{19–26} It is in these contexts that we consider it of interest to investigate the photophysics and photochemistry of cyanoacetylene in the VUV.

Using photoelectron-photoion coincidence techniques we study the photoionization of cyanoacetylene using synchrotron radiation as excitation source over the non-dissociative ionization excitation range 11–15.5 eV. The absolute ionization cross-sections were measured, ionization quantum yields were evaluated, and new spectroscopic features of electronic states of the parent ion were observed and analysed. Structured autoionization features were observed in the total ion yield (TIY) spectrum and were assigned to Rydberg series converging to excited states of HC_3N^+ and to valence shell transitions of cyanoacetylene. Analysis of the experimental observations was aided by quantum chemical calculations of structural and dynamic properties of the cation. Our theoretical results and analyses also led to new information on H-loss dissociation in the ground and excited states of HC_3N^+ .

II. EXPERIMENTAL

Cyanoacetylene was synthesized following the procedure described initially by Moureu and Bongrand¹ and later modified.²⁷ It is a gaseous compound at ambient temperature (T_{amb}). In order to avoid polymerisation it must be stored at low pressure and/or diluted with a rare gas at T_{amb} . For our measurements, the gas is let into a 1 litre stainless steel recipient to attain a pressure $p(\text{HC}_3\text{N}) = 50$ mbar. Helium is added to yield a total pressure $p_{\text{TOT}} \approx 3$ bar. Propane (C_3H_8) is also added to this mixture at the same partial pressure of HC_3N , i.e., $p(\text{C}_3\text{H}_8) = 50$ mbar in order to measure absolute ionization cross-sections according to the comparative method described by Cool *et al.*²⁸ and using the propane cross-section data given by Kameta *et al.*²⁹ and by Wang *et al.*³⁰ All pressures are measured with a Baratron (MKS). The absolute error of this transducer is estimated to be about $\pm 3\%$. Due to the proximity of masses m/z 51 (HC_3N^+) and m/z 44 (propane C_3H_8^+) and the high extraction field used, we consider that the total experimental transmission plus detection efficiency will be the same for both ions.

The recipient is directly connected to a molecular beam inlet using a pressure-reducing regulator. The stagnation pres-

sure was such that only a small signal of the $(\text{HC}_3\text{N})_2$ dimer was detected in the molecular beam, corresponding to 0.4% of the parent, and therefore we consider its contribution to the HC_3N^+ signal via dissociative ionization to be negligible.

Measurements were performed at the undulator beamline DESIRS³¹ of the synchrotron radiation (SR) facility SOLEIL (St. Aubin, France). This beamline incorporates a 6.65 m normal incidence monochromator. For our measurements, we used the 200 grooves/mm grating which provides a constant linear dispersion of 7.2 Å/mm at the exit slit of the monochromator. The typical slit width used in our experiments is 100 μm , yielding a monochromator resolution of 0.7 Å under these conditions (about 6 meV at $h\nu = 10$ eV and 18 meV at $h\nu = 18$ eV). The beamline is equipped with a gas filter³² that effectively removes all the high harmonics generated by the undulator which could be transmitted by the grating. In this work argon was used as a filter gas for all measurements below 15.75 eV. Absorption lines of the rare gas filter occur in the spectra and serve to calibrate the energy scale to an absolute precision of about 4 meV. All the data were normalized with respect to the incoming photon flux, continuously measured by a photodiode (AXUV100, IRD).

The VUV output of this monochromator is directed to the permanent end station SAPHIRS which consists of a molecular beam inlet and an electron-ion coincidence spectrometer called DELICIOUS II. The latter has been described in detail.³³ A brief description is given here: The monochromatized SR beam (200 μm horizontal \times 100 μm vertical extension) is crossed at a right angle with the molecular beam at the centre of DELICIOUS II which combines a photoelectron velocity map imaging (VMI) spectrometer with a linear time-of-flight mass analyzer operating according to Wiley-MacLaren space focusing conditions. The spectrometer is capable of photoelectron/photoion coincidence (PEPICO) measurements where photoelectron images can be recorded for a chosen ion mass. The electron images can be treated to obtain threshold photoelectron spectra of the selected cation, and reveal its electronic structure via the Slow Photoelectron Spectroscopy (SPES) method, which has been described in Refs. 34 and 35 and will also be discussed in Sec. V A. In addition, total ion yields (TIY) as a function of photon energy can be acquired where the spectral resolution is defined only by the slit widths of the monochromator (see above).

III. THEORETICAL CALCULATIONS

Quantum chemical calculations of cyanoacetylene cation electronic state geometries, vibrational frequencies, and electronic state energies were carried out. The quantum chemical calculations were performed using the Molpro code.³⁶ Molecular geometries of neutral and cationic cyanoacetylene as well as the vibrational frequencies were optimized using the coupled cluster technique, including perturbative treatment of triple excitations (CCSD(T)) methods.^{37,38} DFT calculations of geometrical parameters and vibrational modes were also performed using the PBE0 exchange-correlation functional³⁹ with the aug-cc-pvtz basis set. As shown in Tables I and II, DFT calculations reproduce reasonably well

TABLE I. Bondlengths in neutral cyanoacetylene and its cation (present calculation values in bold).

Species	$r(\text{N}\equiv\text{C})$ (Å)	$r(\text{C}\equiv\text{C})$ (Å)	$r(\text{C}-\text{C})$ (Å)	$r(\text{C}-\text{H})$ (Å)	Method
HCCCN $X^1\Sigma^+$	1.157	1.203	1.382	1.057	Expt. ^{46a}
HCCCN $X^1\Sigma^+$	1.1585	1.2054	1.3773	1.0574	Expt. ^{46b}
HCCCN $X^1\Sigma^+$	1.159	1.205	1.378	1.058	Expt. ⁴⁷
HCCCN $X^1\Sigma^+$	1.15853	1.2033	1.3786	1.069	Expt. ⁴⁸
HCCCN $X^1\Sigma^+$	1.164	1.202	1.370	1.054	Calc. ⁵⁰
HCCCN $X^1\Sigma^+$	1.1605	1.2058	1.3764	1.0624	Calc. ⁵¹
HCCCN $X^1\Sigma^+$	1.155	1.201	1.368	1.062	Calc. ⁵²
HCCCN $X^1\Sigma^+$	1.182	1.218	1.372	1.062	Calc. ⁵³
HCCCN $X^1\Sigma^+$	1.18	1.22	1.37	1.07	Calc. ⁵⁴
HCCCN $X^1\Sigma^+$	1.1624	1.2080	1.3803	1.0640	Calc. present ^c
HCCCN $X^1\Sigma^+$	1.1541	1.2006	1.3686	1.0648	Calc. present ^d
HCCCN + $X^2\Pi$	1.1973	1.2465	1.3394	1.0838	Calc. ⁵⁵
HCCCN + $X^2\Pi$	1.188	1.237	1.328	1.067	Calc. ⁵⁰
HCCCN + $X^2\Pi$	1.181	1.233	1.334	1.077	Calc. ⁵⁶
HCCCN + $X^2\Pi$	1.1555	1.2128	1.3524	1.0724	Calc. present ^c
HCCCN + $X^2\Pi$	1.1795	1.2333	1.3327	1.0789	Calc. present ^d
HCCCN + $A^2\Sigma^+$	1.149	1.207	1.340	1.061	Calc. ⁵⁰
HCCCN + $A^2\Sigma^+$	1.1346	1.201	1.3615	1.0736	Calc. present ^d
HCCCN + $B^2\Pi$	1.224	1.227	1.375	1.064	Calc. ⁵⁰
HCCCN + $B^2\Pi$	1.1832	1.2177	1.4294	1.0763	Calc. present ^d
HCCCN + $C^2\Sigma^+$	1.1827	1.2275	1.4163	1.0776	Calc. present ^d

^a r_0 structure.^b r_s structure.^cCCSD(T)/AVTZ calculation.^dPBE0/AVTZ calculation.

the experimental and *ab initio* values of vibrational frequencies and geometrical parameters of the ground state of the cyanoacetylene cation. For this reason the DFT PBE0/AVTZ method was used for geometrical optimization and frequency calculations of the excited electronic states of the ion instead of the CCSD(T)/AVTZ method which is more time consuming. Electronic structure calculations were performed in the C_{2v} point group since the Molpro program does not allow calculations to be done in $C_{\infty v}$ symmetry. The first step is a RHF (Restricted Hartree-Fock) calculation of the electronic ground state of the HCCCN⁺ cation. Then, the electronic structure computations were performed using the full valence complete active space self-consistent field (CASSCF) approach^{40,41} followed by the internally contracted multi-reference configuration interaction (MRCI).⁴² We employed the aug-cc-pvtz (augmented correlation consistent polarized valence triple zeta) basis set of Dunning⁴³ for the carbon, nitrogen, and hydrogen atoms.

The adiabatic ionization energy of cyanoacetylene was calculated by DFT/PBE0 and CCSD(T) methods, which gave good agreement with experimental values (Appendix A, Table VIII). Vertical ionization energies were calculated by both MRCI and CASSCF techniques. The results of calculations at the CASSCF/AVTZ level of theory reproduce quite well the electronic state energies of the cation (see Appendix A, Table IX). For this reason the less time-consuming method, CASSCF/AVTZ, was used for calculation of one-dimensional cuts of the potential energy surfaces of the ground and first three electronic excited doublet states of the HCCCN⁺ cation along the C–H elongation pathway leading to H-loss (see

Sec. IV D). Further details of the theoretical calculations and results are given in Appendix A.

IV. ELECTRONIC, VIBRATIONAL, AND GEOMETRIC STRUCTURAL PRELIMINARIES

In order to interpret the results of experiments described in Sec. II it is useful to present here information on the electronic, vibrational, and geometrical structures of neutral and ionic cyanoacetylene.

A. Electronic structure

Experimental HeI and HeII photoelectron spectra of cyanoacetylene and assignments reported by Baker and Turner⁴⁴ and Åsbrink *et al.*⁴⁵ have provided the following successive ionization energies and assigned molecular orbital symmetries corresponding to the ejected electrons: 11.60 eV 2π , 13.54 eV 9σ , 14.03 eV 1π , 17.62 eV 8σ , thus giving the electron configuration corresponding to the ground state of the cyanoacetylene ion as: ... $8\sigma^2 1\pi^4 9\sigma^2 2\pi^3 X^2\Pi$. The M.O. assignments were mainly based on calculations both in Koopmans' approximation and by an *ab initio* many-body Green's function method.

B. Geometry

The geometrical structure of neutral cyanoacetylene has been determined by microwave (MW) spectroscopy.^{46,47} A

TABLE II. Vibrational frequencies (cm^{-1}) in neutral and ionic electronic states of cyanoacetylene. Present results are in bold italics. The experimental values in Refs. 44, 58, and 59 have a $\pm 50 \text{ cm}^{-1}$ error bar.

Vibration	Neutral $X^1\Sigma^+$ ^a	Ion $X^2\Pi$	Ion $A^2\Sigma^+$	Ion $B^2\Pi$	Ion $C^2\Sigma^+$
$\nu_1(\text{C-H})$	3327	3196.5 ⁵⁷	3186	3130	1320 ⁴⁴
	3312 ⁵⁷	3105	3401 calc. ^c	3366 calc. ^c	3347 calc. ^c
	3344 calc. ^b	3265 calc. ⁵⁵			
	3472 calc. ^c	3326 calc. ⁵⁶			
$\nu_2(\text{C}\equiv\text{N})$	2271	2175.8 ⁵⁷	2291	1940 ⁴⁴	2232 calc. ^c
	2285 calc. ^b	2180 ^{44,58}	2343 calc. ^c	2033	
	2398 calc. ^c	2185		2229 calc. ^c	
		2179 calc. ⁵⁵			
		2261 calc. ⁵⁶			
		2250 calc. ^b			
$\nu_3(\text{C}\equiv\text{C})$	2077	1852.8 ⁵⁷	2057	1742	2068 calc. ^c
	2085 calc. ^b	≈ 1830	2240 calc. ^c	2153 calc. ^c	
	2191 calc. ^c	1869 calc. ⁵⁵			
		1934 calc. ⁵⁶			
		2097 calc. ^b			
$\nu_4(\text{C-C})$	876	820 ⁵⁹	860 ⁴⁴	810 ⁴⁴	824 calc. ^c
	863.5 ⁴⁹	877 ⁵⁸	895	820 (871) ⁵⁹	
	870 calc. ^b	906 calc. ⁵⁵	921 calc. ^c	774	
	910 calc. ^c	893 calc. ⁵⁷		820 calc. ^c	
		933 calc. ⁵⁶			
		890 calc. ^b			
		941 calc. ^c			
ν_5	663	715 calc. ⁵⁷	833 calc. ^c	789 [see text]	730 calc. ^c
	663.2 ⁴⁹	715 calc. ^b		783 calc. ^c	
	677 calc. ^b	704 calc. ^c			
	715 calc. ^c				
ν_6	500	411	347–451	520 [see text]	568 calc. ^c
	498.5 ⁴⁹	528 calc. ^b	590 calc. ^c	459	
	507 calc. ^b	521 calc. ^c		490 calc. ^c	
	551 calc. ^c				
ν_7	224	198 calc. ^b	208 calc. ^c	147 [see text]	226 calc. ^c
	222.4 ⁴⁹	218 calc. ^c		220 calc. ^c	
	250 calc. ^b				
	241 calc. ^c				

^aNeutral molecule ground state data, mainly by IR and Raman studies, from Refs. 91–93 unless otherwise indicated.^bCCSD(T)/aug-cc-pvtz calculation of harmonic vibrational frequencies.^cPBE0/aug-cc-pvtz calculation of harmonic vibrational frequencies.

further refined analysis of the experimental data was carried out by Watson *et al.*,⁴⁸ who used as data not only those of Tyler and Sheridan⁴⁷ but also of Mallinson and de Zafra⁴⁹ who had studied MW spectra (and mm wave spectra for vibrationally excited states) of 10 isotopologues of HC_3N .

As expected from its electronic structure, cyanoacetylene is a linear molecule; its bond lengths as determined by Tyler and Sheridan⁴⁷ are $r(\text{N}\equiv\text{C}) = 1.159 \text{ \AA}$, $r(\text{C}\equiv\text{C}) = 1.205 \text{ \AA}$, $r(\text{C-C}) = 1.378 \text{ \AA}$, $r(\text{C-H}) = 1.058 \text{ \AA}$. There are no direct determinations of the bond lengths in the ion but we can compare values of both neutral and ion ground state bond lengths, calculated by a variety of theoretical methods. Table I, which gives the relevant data, includes the results

of our *ab initio* calculations. The calculated internuclear distances of neutral cyanoacetylene ground state in Table I are mainly in good agreement with experiment. Although the calculated bondlengths of the $X^2\Pi$ ground state of the ion differ by 1%–2% in our own and the three^{50,55,56} reported calculations, these ion state values in Table I are sufficiently different from those of the neutral molecule to allow us to validly compare the ion bondlengths with those of the neutral. This shows that in going from the neutral to the ion ground state $r(\text{N}\equiv\text{C})$ increases by about 2%–3%, $r(\text{C}\equiv\text{C})$ increases by about 3% and $r(\text{C-C})$ decreases by about 3%–4%, whereas in going to the $A^2\Sigma^+$ first excited state of the ion $r(\text{N}\equiv\text{C})$ decreases by about 2%, $r(\text{C}\equiv\text{C})$ remains basically unchanged

and $r(\text{C}-\text{C})$ decreases by about 1%–2%. Excitation to the $\text{B}^2\Pi$ state also modifies the internuclear bondlengths: $r(\text{N}\equiv\text{C})$ increases by 3%–5%, $r(\text{C}\equiv\text{C})$ increases about by 1%–2% and $r(\text{C}-\text{C})$ possibly remains basically unchanged (0%–3% increase). The bondlength changes in excitation to the $\text{C}^2\Sigma^+$ state are similar to the $\text{B}^2\Pi$ case, according to our calculations. The C–H bond appears to be relatively little affected in these various ionization processes since changes in $r(\text{C}-\text{H})$ appear to be at most increases of about 1% in formation of the $\text{X}^2\Pi$, $\text{A}^2\Sigma^+$, $\text{B}^2\Pi$, and $\text{C}^2\Sigma^+$ ion states.

This comparison of ground state neutral and ion corresponding bondlengths indicates that on forming the cyanoacetylene ion ground state the CN and CC stretching vibrations are likely to be excited and, furthermore, that the $\text{N}\equiv\text{C}$ and $\text{C}\equiv\text{C}$ bonds should acquire some measure of double bond character, thus increasing the tendency to linear structure as exemplified in cumulenes. This, and excitation to the excited states of the ion, will be further discussed later.

C. Vibrations

Cyanoacetylene has 7 normal vibrations: 4 stretching vibrations (modes 1–4) of σ symmetry and 3 doubly degenerate bending vibrations (modes 5–7) of π symmetry. The frequencies of the ground state vibrations are well known from IR and Raman studies (Table II). Corresponding data for the cation electronic states are known from a variety of optical spectroscopy and photoelectron spectroscopy studies as well as some theoretical calculations, including our own by methods discussed in Sec. III and Appendix A. These vibrational frequency values and the corresponding references of work previous to the present study are listed in Table II. Vibrational aspects of the ion electronic states as exhibited in the PEPICO (TIY) and SPES spectra will be discussed below. The vibrational frequencies resulting from our analysis of the SPES spectra, presented below, are also given in Table II.

V. RESULTS AND DISCUSSION

We first note that the 11–15.6 photoionization energy region explored experimentally in this study is below the first dissociative ionization onset which corresponds to H-atom or N-atom loss process occurring, respectively, at 17.78 ± 0.08 eV and 17.76 ± 0.08 eV.⁶⁰

A. Slow photoelectron spectroscopy (SPES) of the cyanoacetylene parent cation: Analysis and assignments

As mentioned in Sec. II, the spectrometer records mass-selected photoelectron images. These images are then Abel inverted using the pBasex algorithm⁶¹ to yield photoelectron spectra at any and all the photon energies of the scan. The data are displayed in the form of an intensity matrix in Figure 1(a) for the HC_3N^+ parent ion over the 11.3–15.5 eV excitation energy region, where the photoelectron kinetic energy is plotted against the photon excitation energy. This matrix carries

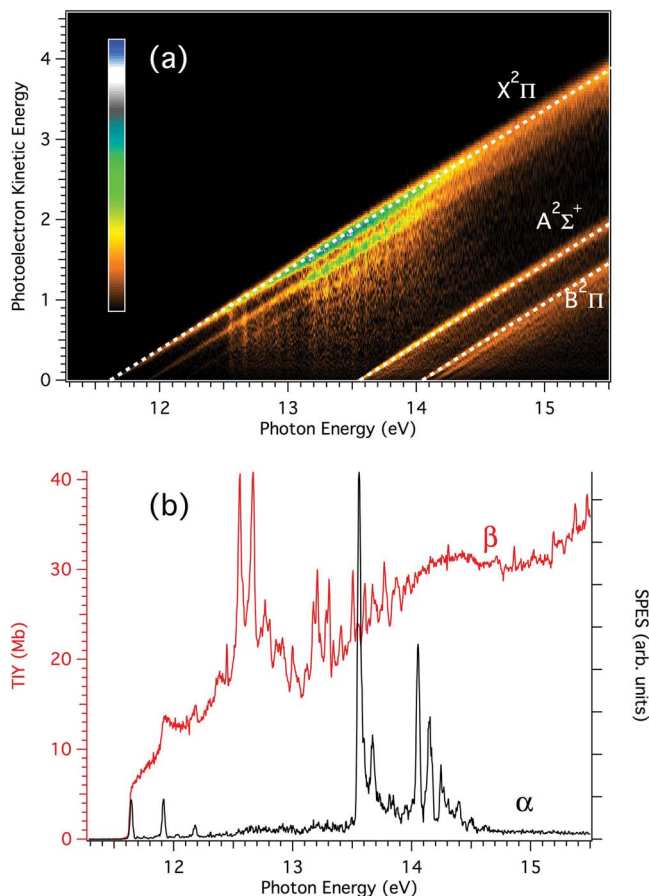


FIG. 1. (a) Photoelectron intensity matrix of cyanoacetylene obtained with an extraction field of 572 V/cm (electron $\text{KE}_{\text{max}} = 5.7$ eV). The white diagonal dashed lines trace the electronic states of the cation. (b) Derived SPES (black curve, α) and ionization cross-section (TIY, red curve, β). Note that the latter is given in absolute units (see text for details).

a wealth of information that can be reduced in various ways. Energy conservation impels those electrons that are ejected into the continuum through a direct ionization process to appear as diagonal lines of constant slope ($h\nu - \text{IE}_i/\text{KE}$), where $h\nu$ is the photon energy, IE_i is the i th state ionization energy, and KE is the photoelectron kinetic energy. As described by Pouilly *et al.*,³⁴ one can now integrate the electron signal along the slope direction up to a certain KE for each photon energy in order to obtain the SPES, which provides cation electronic state spectra with high electron resolution without compromising the signal to noise ratio. The integration range chosen here ($0 < \text{KE} < 50$ meV) yields an electron resolution of ≈ 25 meV.

The resulting SPES for the parent $m/z = 51$ ion are shown in Fig. 1(b) (α) over the range 11.3–15.5 eV. The bands in the 11.3–15.5 eV region have previously been observed by He I⁴⁴ and He II⁴⁵ photoelectron spectroscopy.

Three spectral band regions, corresponding to formation of the $\text{X}^2\Pi$, $\text{A}^2\Sigma^+$ and $\text{B}^2\Pi$ ion states can be seen between 11.6 and 14.7 eV. The band energies and assignments are compiled in Table III. Graphical zooms of the regions of interest given in Figure 2 include band assignments that are presented below. It is of interest that the $\text{X}^2\Pi$ state region in the SPES spectrum is much less intense, relative to the $\text{A}^2\Sigma^+$ and

TABLE III. HC₃N SPES : Band energies and assignments.

Band No.	Energy (eV)	Energy (cm ⁻¹)	Assignment	Vibrational frequencies ν (cm ⁻¹)
1	11.573 ^a	93 342 ^a	X ² Π O ⁰ ₀ adiabatic	
2	11.643	93 907	X ² Π O ⁰ ₀ vertical	
3	11.694	94 318	6 ¹ ₀	$\nu_6 = 411$
4	11.748	94 753	6 ² ₀	$846/2 = 423; \nu_6 = 435$
5	11.914	96 092	2 ¹ ₀	2185
6	12.028	97 012	1 ¹ ₀	3105
7	12.179	98 230	2 ² ₀	$4323/2 = 2162; \nu_2 = 2138$
8	13.557	109 344	A ² Σ ⁺ O ⁰ ₀ vertical	
9	13.600	109 691	6 ¹ ₀	$\nu_6 = 347$
10	13.668	110 239	4 ¹ ₀	$\nu_4 = 895$
11	13.812	111 401	3 ¹ ₀	$\nu_3 = 2057$
12	13.841	111 635	2 ¹ ₀	$\nu_2 = 2291$
13	13.868	111 852	3 ¹ ₀ 6 ¹ ₀	$\nu_6 = 451$
14	13.952	112 530	1 ¹ ₀	$\nu_1 = 3186$
15	14.006	112 965	1 ¹ ₀ 6 ¹ ₀	$\nu_6 = 435$
16	14.053	113 345	B ² Π O ⁰ ₀ vertical	
17	14.149	114 119	4 ¹ ₀	$\nu_4 = 774$
18	14.244	114 885	4 ² ₀	$1540/2 = 770; \nu_4 = 766$
19	14.269	115 087	3 ¹ ₀	$\nu_3 = 1742$
20	14.305	115 378	2 ¹ ₀	$\nu_2 = 2033$
21	14.340	115 659	4 ³ ₀	$2314/3 = 771; \nu_4 = 774$
22	14.397	116 119	2 ¹ ₀ 4 ¹ ₀	$\nu_4 = 741$
23	14.441	116 475	1 ¹ ₀	$\nu_1 = 3130$
24	14.498	116 934	1 ¹ ₀ 6 ¹ ₀	$\nu_6 = 459$
25	14.621	117 926		

^aFrom TIIY spectrum (Sec. V B 2 and Table V).

B²Π state regions, than is observed in HeI⁴⁴ and He II⁴⁵ PES spectra. This is possibly due to the fact that in SPES we measure mainly electrons close to the excitation threshold and that the ionization yield is small in the X²Π state region. Another possible partial contributing factor is the use of argon as a gas filter since there are strong Ar I resonance lines in this energy region which could affect the excitation energy flux at cyanoacetylene absorption wavelengths in this energy region.

1. X²Π ion state region 11.6–12.2 eV

The SPES in the X²Π ion state region is very similar to that of He I PES⁴⁴ but a little better resolved than in previous studies and so more amenable to analysis. In the first region (Fig. 2(a) and Table III) the SPES band peaking at 11.643 eV (FWHM = 180 cm⁻¹) can be considered as the vertical ionization energy IE_v of cyanoacetylene and is thus the O⁰₀ origin band of the X²Π ion state. It is the first of an apparent progression of 3 bands. The successive intervals of 271 meV (2185 cm⁻¹) and 265 meV (2137 cm⁻¹) between, respectively, the first two and the second two bands in this progression can be assigned to the ν_2 (C≡N) stretching vibration whose previously reported ion ground state frequency experimental values are 2180 ± 40 cm⁻¹ from He I PES⁴⁶ and, in a Ne matrix, 2176 cm⁻¹¹⁵⁷ [Table II]. The changes in the C≡N bondlength on ionization (Table I) make it likely, Franck-Condon-wise, that ν_2 (C≡N) will be excited.

In this first region there is also a weak feature, at 12.028 eV, that is 385 meV (3105 cm⁻¹) from the X²Π O⁰₀ band. This feature was not previously reported in PES studies. Examination shows that it is apparently hidden in the noise in published PES spectra^{44,45} as compared with our much better signal/noise SPES spectrum. The band interval of 3105 cm⁻¹ can reasonably be considered to be the ν_1 (C–H) stretch vibration frequency whose ion ground state value has been calculated to be of this magnitude and whose experimental value in a Ne matrix is 3196.5 cm⁻¹ (Table II). The excitation of a weak ν_1 (C–H) feature on ionization of cyanoacetylene is to be expected from the calculated minor lengthening of the C–H bond (Table I).

Two more very weak features, not previously reported, occur at 11.694 and 11.748 eV in the X²Π ion ground state portion of the SPES (Fig. 2(a)). These features have successive intervals of 411 and 435 cm⁻¹. They are, respectively, assigned as the 6¹₀ and 6²₀ vibronic bands (Table III). The mode ν_6 is a bending vibration whose neutral ground state frequency is 498.5 cm⁻¹ (Table II). Its decrease in the X²Π ion state is consistent with the increase of the N≡C and C≡C bondlengths and the shortening of the C–C bondlength (Table I) that collectively indicate a tendency towards a cumulene structure in the X²Π ion state. The excitation of a bending vibration on ionization has also been observed as weak features in the SPES of dicyanoacetylene.⁴

The geometrical changes on ionization of cyanoacetylene discussed above indicate that on ionization to the X²Π ion

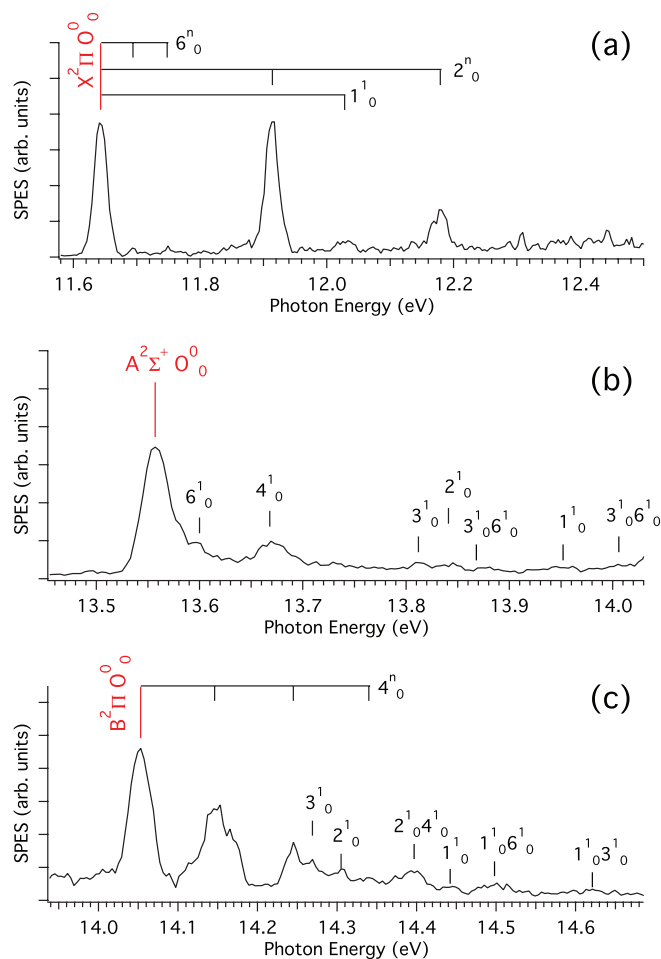


FIG. 2. SPES spectra of cyanoacetylene and proposed assignments: (a) 11.6–12.5 eV, (b) 13.5–14.0 eV, (c) 14.0–14.7 eV.

ground state one might also expect to excite the $\nu_3(\text{C}\equiv\text{C})$ stretching vibration by virtue of the lengthening of $r(\text{C}\equiv\text{C})$ on ionization. A corresponding SPES feature is not observed as a clearly defined peak but can be suspected to exist as the very weak broad signal around 11.870 eV (Fig. 2(a)) corresponding to $\nu_3(\text{C}\equiv\text{C}) \approx 1830 \text{ cm}^{-1}$; a calculated value is 1869 cm^{-1} and a Ne matrix experimental value is 1852.8 cm^{-1} (Table II).

The SPES region between 12.5 and 13.5 eV is marked by a large number of irregular weak features. We consider them to be related to the strong autoionization features in the TIIY spectrum (Fig. 1(b), cf. spectra α and β) rather than being instrumental noise.

2. The $\text{A}^2\Sigma^+$ ion state region 13.5–14.0 eV

In the second SPES region, between 13.5 and 14.0 eV (Fig. 2(b)) the bands are essentially the same as previously observed in He I PES by Baker and Turner⁴⁴ and Kreile *et al.*,⁶² as well as in the He II spectra of Asbrink *et al.*⁴⁵ They arise by electron ejection from the 9σ M.O to form the $\text{A}^2\Sigma^+$ ion state whose O^0_0 band (vertical energy) we observe at 13.557 eV, in agreement with the PES value of 13.54 eV.^{44,45} The vibrational structure, which appears to be somewhat irregular, is better resolved than in published PES spectra. Vibrational

progressions appear to be limited to a single member. Our analysis, given in Table III, is more extensive than that of Baker and Turner, who assigned only one vibration, ν_4 , in the $\text{A}^2\Sigma^+$ ion state.⁴⁴

Only one member of a C–C stretch progression in ν_4 (C–C stretch) = 895 cm^{-1} is found, corresponding to the band at 13.668 eV, observed also by Baker and Turner,⁴⁴ who give the ν_4 frequency as $860 \pm 40 \text{ cm}^{-1}$. Our value is about 4% greater than that of the neutral cyanoacetylene ground state value, 864 cm^{-1} (Table II), which is consistent with the decrease in $r(\text{C–C})$ on ionization to the $\text{A}^2\Sigma^+$ state.

Assignments to other bands in the $\text{A}^2\Sigma^+$ ion state region (the bands in the 13.83–14 eV region are more easily discernable in Fig. 1(b) α than in the energy expanded version of Fig. 2) are as follows:

- The 6^1_0 band at 13.600 eV, giving $\nu_6 = 347 \text{ cm}^{-1}$. This value is much lower than that observed in the $\text{X}^2\Pi$ ion state.
- The 3^1_0 band at 13.812 eV which provides $\nu_3(\text{C}\equiv\text{C}) = 2057 \text{ cm}^{-1}$, similar to the frequency $\nu_3 = 2077 \text{ cm}^{-1}$ of the neutral ground state vibration. This is consistent with $r(\text{C}\equiv\text{C})$ being virtually unchanged on $\text{A}^2\Sigma^+$ state ionization (Table I).
- The 2^1_0 band at 13.841 eV that corresponds to $\nu_2(\text{C}\equiv\text{N}) = 2291 \text{ cm}^{-1}$. This is slightly greater than the neutral ground state value, $\nu_2(\text{C}\equiv\text{N}) = 2271 \text{ cm}^{-1}$, and is consistent with a calculated decrease in $r(\text{C}\equiv\text{N})$ in the $\text{A}^2\Sigma^+$ ion state as compared with the value in the neutral species (Table I).
- The 1^1_0 band at 13.952 eV which corresponds to $\nu_1(\text{C–H}) = 3186 \text{ cm}^{-1}$. The 4% decrease in frequency as compared with the value in the neutral ground state (Table II) is consistent with our PBE0/AVTZ $r(\text{C–H})$ calculations (Table I), and also with the *ab initio* calculations of Mendes *et al.*⁵⁰

The spectral structure irregularities in this spectral region are reminiscent of vibronic interactions but the situation is not clear and merits theoretical investigation, including the possibility of interaction between the $\text{A}^2\Sigma^+$ state and quartet states. In this respect it is of interest to mention two observational results: (i) absorption spectra of HC_3N^+ in a Ne matrix have no features corresponding to the $\text{A}^2\Sigma^+ \leftarrow \text{X}^2\Pi$ transition, although the $\text{B}^2\Pi \leftarrow \text{X}^2\Pi$ transition was observed.⁵⁹ This is consistent with the finding that in most acetylenic cations the $\sigma^{-1} \leftrightarrow \pi^{-1}$ optical transitions have oscillator strengths that are an order of magnitude lower than for $\pi^{-1} \leftrightarrow \pi^{-1}$ transitions;⁵⁹ (ii) $\text{A}^2\Sigma^+ \rightarrow \text{X}^2\Pi$ emission of HC_3N^+ is not observed in the gas phase⁶³ in spite of the fact that the first dissociation limit is at a much higher energy than the $\text{A}^2\Sigma^+$ state. This provides evidence for fast internal conversion from $\text{A}^2\Sigma^+$ either directly by vibronic coupling to high vibrational levels of the ground state of the ion, similar to the case of the acetylene ion,⁶⁴ or possibly via a quartet state. In the case of the related species, the diacetylene cation, calculations⁶⁵ demonstrate the likely existence of quartet states that lie close to the minimum energy of the first electronic excited state, $\text{A}^2\Sigma_u^+$, which is the state corresponding to $\text{A}^2\Sigma^+$ in HC_3N^+ . Vibronic coupling effects

TABLE IV. $\text{HC}_3\text{N}^+ \text{B}^2\Pi \leftarrow \text{X}^2\Pi$ absorption transition: Ne matrix spectral features in Fig. 2 of Fulara *et al.*⁵⁹

λ (Å) [Fu] ^a	ν (cm ⁻¹) [Fu]	Assignment [Fu]	λ (Å) [Pr] ^b	ν (cm ⁻¹) [Pr]	Present assignment
5160	19 374	O ⁰ ₀	5159	19 384	O ⁰ ₀
5124	19 511	7 ¹ ₀	5120	19 531	7 ¹ ₀ : $\nu_7 = 147 \text{ cm}^{-1}$
			5024	19 904	6 ¹ ₀ : $\nu_6 = 520 \text{ cm}^{-1}$
			4957 (sh) ^c	20 173	5 ¹ ₀ : $\nu_5 = 789 \text{ cm}^{-1}$
4938	20 245	4 ¹ ₀	4935	20 263	4 ¹ ₀ : $\nu_4 = 879 \text{ cm}^{-1}$
			4832.5	20 693	5 ¹ ₀ 6 ¹ ₀ : $\nu_6 = 520 \text{ cm}^{-1}$
4746	21 064	4 ² ₀	4743	21 084	4 ² ₀

^aFu = Values and assignments reported by Fulara *et al.*⁵⁹^bPr = Present measurements of Fig. 2 features of Fulara *et al.*⁵⁹^csh = shoulder.

could indeed be responsible for the apparent irregularities in our SPES spectra.

3. The B²Π ion state region 14.0–14.7 eV

The third SPES region, 14.0–14.7 eV has vibronic features corresponding to the B²Π ion state. The origin band is at 14.053 eV (Table III), in fair agreement with the 14.03 eV PES value of Baker and Turner.⁴⁴ Vibrational structure in the HeI PES has been assigned by Baker and Turner to two regular progressions involving the excitation of two vibrations $\nu_2(\text{C}\equiv\text{N}) = 1940 \pm 40 \text{ cm}^{-1}$ and $\nu_4(\text{C}-\text{C}) = 810 \pm 40 \text{ cm}^{-1}$. In our B²Π state SPES region the vibrational features appear to be more irregular than would be expected from the Baker-Turner assignments. However, close inspection of the Baker-Turner PES⁴⁴ confirms the somewhat irregular spacings of the vibrational features we observe in our SPES in this spectral region (Table III). Our values for the two vibrations assigned by Baker and Turner are $\nu_2(\text{C}\equiv\text{N}) = 2033 \text{ cm}^{-1}$ and $\nu_4(\text{C}-\text{C}) = 774 \text{ cm}^{-1}$. The lowering of $\nu_2(\text{C}\equiv\text{N})$ and $\nu_4(\text{C}-\text{C})$ with respect to their neutral ground state values (Table II) is consistent with the bondlength changes on ionization to the B²Π ion state (Table I).

Two other vibrations are assigned in our B²Π region SPES spectrum, $\nu_1(\text{C}-\text{H}) = 3130 \text{ cm}^{-1}$, whose value is consistent with the calculated 1% increase in $r(\text{C}-\text{H})$ (Table I), and $\nu_3(\text{C}\equiv\text{C}) = 1742 \text{ cm}^{-1}$, which is also consistent with bondlength changes on ionization to the B²Π state.

Further information on B²Π state vibrations can be obtained from the Ne matrix absorption spectrum of HC_3N^+ ⁵⁹ containing vibronic bands corresponding to the B²Π \leftarrow X²Π transition and whose visible region features were reported with a precision of $\pm 10 \text{ Å}$ ($\pm 4.7 \text{ meV}$). The Fulara *et al.* assignment of the absorption band at 5160 Å to the O⁰₀ origin transition⁵⁹ leads to a B²Π – X²Π energy difference of 2.402 eV, whereas our SPES spectrum provides a value of 2.410 eV. Taking into account the precision of our SPES measurements, this would represent a Ne matrix shift nominally of $8 \pm 9 \text{ meV}$, which is consistent with the less than 30 meV previously observed for Ne matrix shifts of electronic transitions of molecular ions.⁶⁶ The SPES band at 14.149 eV, at 774 cm^{-1} above the B²Π O⁰₀ feature, corresponds within 5 meV to the $\Delta E = 2.501 \text{ eV}$ energy of the strong absorption band at 4938 Å assigned by Fulara *et al.* as 4¹₀,

where $\nu_4(\text{C}-\text{C stretch}) = 871 \text{ cm}^{-1}$ but is reported as $820 \pm 60 \text{ cm}^{-1}$.⁵⁹ Our value of $\nu_4 = 774 \text{ cm}^{-1}$ is in agreement with that of Baker and Turner, $810 \pm 45 \text{ cm}^{-1}$.⁴⁴

Using the published Ne matrix absorption spectrum of HC_3N^+ (Fig. 2 of Fulara *et al.*⁵⁹) we measured a set of seven features, including three not previously reported by Fulara *et al.*⁵⁹ although they are clearly present on their absorption spectrum. A comparison between our measurements and those reported by Fulara *et al.* is given, with assignments, in Table IV. The previous assignments of Fulara *et al.* are to the 4¹₀, 4²₀, and 7¹₀ features, with which we concur but remark the discrepancy between the values of ν_4 in the Ne matrix and our gas phase SPES spectrum, possibly due to matrix effects on vibronic coupling phenomena. New vibrational frequencies are those of the bending vibrations $\nu_5 = 789 \text{ cm}^{-1}$ and $\nu_6 = 520 \text{ cm}^{-1}$. The relative importance of these bending vibrations could also result from vibronic interactions. However, further work, both experimental and theoretical, is required to validate the proposed assignments of the absorption spectrum.

B. TIY spectra of the cyanoacetylene parent cation: Analysis and assignments

Integration of all the photoelectron kinetic energies as a function of the photon energy, performed on the photoelectron matrix in Figure 1(a), gives the Total Ion Yield (TIY) spectrum of the parent ion, plotted in Figure 1(b) β between 11.6 and 15.5 eV and presented in more detail in Figure 3 for the region 12.2–15.6 eV. Before presenting the analysis of this spectrum we first discuss the determination of the photoionization cross-sections and estimation of ionization quantum yields.

1. Ionization cross-sections and quantum yields

a. Calibration of ionization cross-sections. In Sec. II we mentioned that our cyanoacetylene ionization cross-sections were determined by a calibration method²⁸ based on the ionization cross-sections of propane. Recent measurements of the ionization cross sections (σ_{ion}) of propane are by two different groups Kameta *et al.*²⁹ and Wang *et al.*³⁰ Kameta *et al.* used an absolute method to determine σ_{ion} of propane whereas Wang *et al.* employed a relative method. This method, described by Cool *et al.*,²⁸ is based on the σ_{ion}

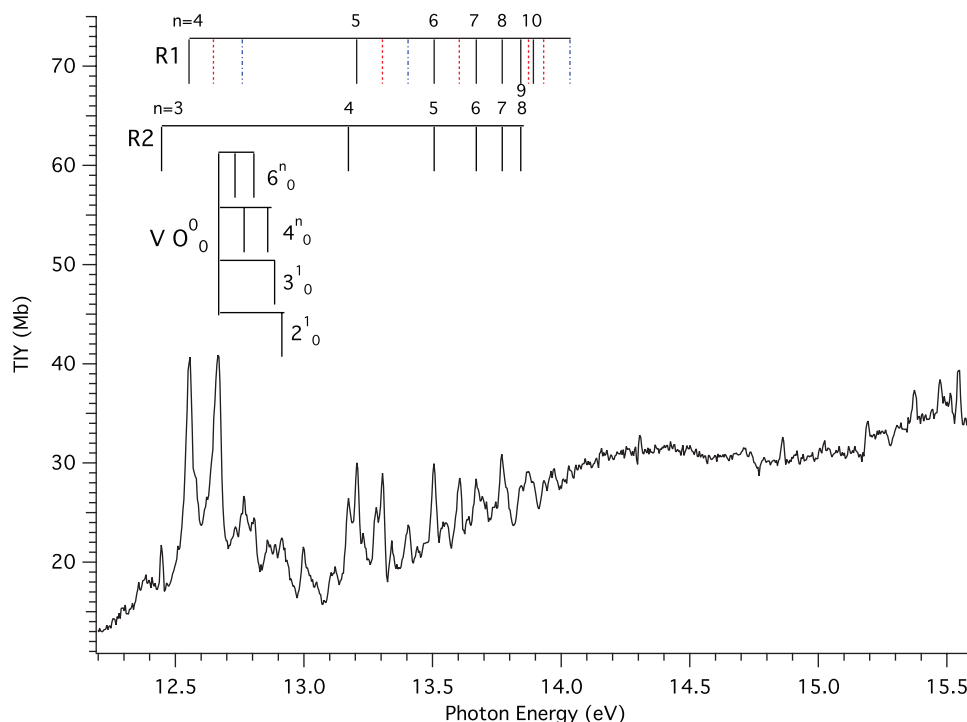


FIG. 3. Total ion yield spectrum of the cyanoacetylene ion, m/z 51: 12.2–15.6 eV. The vertical red (blue) dashed (point-dashed) lines represent 4^1_0 (4^2_0) excitations having a R1 Rydberg series member as origin. V = Valence transitions.

of propene as a standard which is stated to have been accurately measured by Person and Nicole in 1970.⁶⁷ The propane ion yield curve of Kameta *et al.* differs by a varying factor of 2.0–1.2 from that of Wang *et al.* over the energy range 11.6–12.5 eV. This difference cannot be easily explained.

In view of the importance of valid calibration we compared our own propane ionization yield curve with that of Wang *et al.* (Fig. 4). In this figure is plotted the ratio of our measured propane ion yields to those of Wang *et al.*³⁰ as a function of photon excitation energy between 11.6 and 12.5 eV. The average value (solid line) was then applied for absolute normalisation. The dispersion of the data is rather

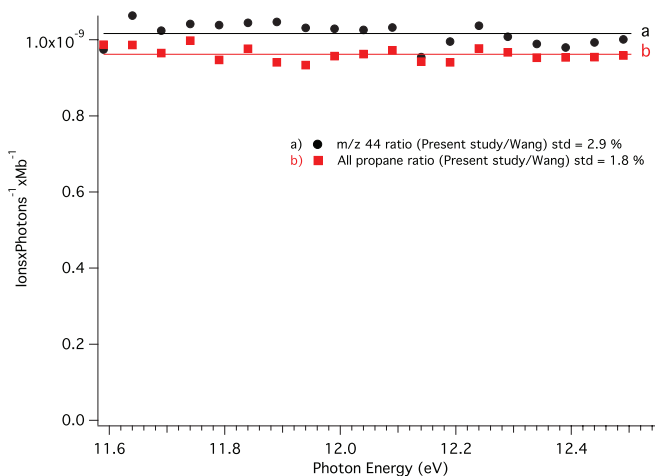


FIG. 4. Photoionization cross-sections σ_i of propane between 11.6 and 12.5 eV: Ratio of σ_i (present study)/ σ_i (Wang *et al.*³⁰) for (a) m/z 44 and (b) Σ (all ions, m/z 44,43,42,29,28).

random, and the average values are close together (to within 5%) whether just the propane m/z 44 curve, or the sum of all the propane masses (m/z 44, 43, 42, 29, 28) is chosen. Since there is such a good agreement between the slopes in Wang *et al.* and our work, this implies that the shape of the Kameta *et al.* propane ion yield curve in the ionization onset region is incorrect, and thus also their absolute cross-sections.

The constancy of the intensity ratio in Figure 4, to within an error of about 2.9% in the excitation energy region 11.59–12.49 eV, leads us to prefer calibration with the propane data of Wang *et al.* These observations do not prove that the absolute values of Wang *et al.* are correct, but they show the need for further studies on the ion yield curve of propane in order to remove the calibration ambiguities which can occur, and no doubt have occurred, through use of the Kameta *et al.* and the Wang *et al.* ionization cross-section data in previous studies.

b. Photoionization cross-section and quantum yields. In Figure 5 we show the cyanoacetylene absorption spectrum (Fig. 5(a)), measured earlier,⁶⁸ and our absolute TIY spectrum whose ionization cross sections were calibrated using the propane data from both Wang *et al.*³⁰ (Fig. 5(b)) and Kameta *et al.*²⁹ (Fig. 5(c)). Calibration with Kameta *et al.* was restricted to the cross-section value at 11.65 eV, so that the cyanoacetylene ion yield curves b and c in Fig. 5 consequently differ by a constant factor of 2 in the cross-section values. Except in the immediate ionization threshold region, the TIY spectrum is closely similar to, but better resolved than, the VUV absorption spectrum of Ferradaz *et al.*⁶⁸ in the same energy region.

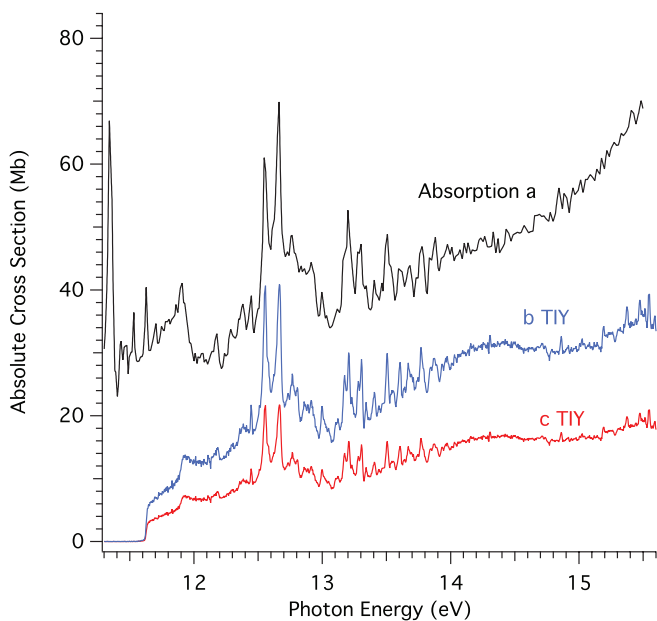


FIG. 5. Cyanoacetylene: comparison between the VUV absorption spectrum (a)⁷⁶ and the total ion yield spectrum obtained using propane ionization cross-section values from Wang *et al.*³⁰ (b) and Kameta *et al.*²⁹ (c) (see text for details).

We can estimate the ionization quantum yield Φ_i at specific excitation energies by application of a rule of thumb⁶⁹ which states that, especially in the case of large polyatomic molecules, the ionization quantum yield Φ_i tends to become a quasi-linear function of excitation energy in a range up to ≈ 9.2 eV above the ionization energy, where it reaches $\Phi_i \approx 100\%$. This can be also be demonstrated by integration of HeI photoelectron spectra.⁷⁰ On the basis of this rule of thumb⁶⁹ we estimate the ionization quantum yield of cyanoacetylene to be about 37% at $E_{\text{exc}} \approx 15$ eV, so that about 63% of the photon excitation would be to non-autoionizing superexcited states at this energy. Superexcited states can, in general, undergo a variety of relaxation processes, besides autoionization and dissociative autoionization, such as relaxation from stable or dissociative neutral excited states. This includes participating as reaction intermediates or in collision complexes in electron-ion recombination, electron attachment and Penning ionization.⁷¹

At $E_{\text{exc}} = 15$ eV, which is below the dissociative ionization threshold of cyanoacetylene,⁶⁰ the total ionization cross-section is 16×10^{-18} cm² using the propane cross-section data of Kameta *et al.*²⁹ (Fig. 5). The VUV absorption measurements on cyanoacetylene (Fig. 5(a)) gave 57.3×10^{-18} cm² for the photoabsorption cross-section in the 15 eV region.⁶⁸ The ionization quantum yield at this photon excitation energy is thus 28%. This is smaller than the ionization quantum yield predicted by the rule of thumb of Jochims *et al.*⁶⁹ On the other hand, using σ_{ion} of propane from Wang *et al.*³⁰ we calculate $\Phi_i = 56\%$ at 15 eV, which is higher, by about 20%, than the rule of thumb estimate. At this stage we cannot make a definitive conclusion on Φ_i and further work is required to clarify the inconsistency of propane ionization cross-section data in the literature.

2. Ionization energy of the ground state

From the TIY spectrum of the parent ion HC_3N^+ at $m/z = 51$ (Fig. 1(b) spectrum β) we measure an adiabatic ionization energy $\text{IE}_{\text{ad}}(\text{HC}_3\text{N}) = 11.573 \pm 0.010$ eV. The rise of the ion signal to the onset of a semi-plateau is consistent with $\text{IE}_{\text{vert}} = 11.643$ eV determined from our SPES spectrum (see Sec. V A 1). The difference between the adiabatic and maximum values of the origin band is attributed to the spectrometer's electron kinetic energy resolution and the Franck-Condon overlap between the neutral ground state and ion ground state $v = 0$ levels.

Adiabatic and vertical ionization energies were calculated with various methods (Appendix A). The CCSD(T)AVTZ based calculations, which include zero point vibrational energy (ZPE) corrections, gave $\text{IE}_{\text{ad}}(\text{HC}_3\text{N}) = 11.57$ eV and $\text{IE}_{\text{vert}} = 11.63$ eV, in excellent agreement with our experimental values, while the results of DFT/PBE0 calculations, $\text{IE}_{\text{ad}}(\text{HC}_3\text{N}) = 11.30$ eV and $\text{IE}_{\text{vert}} = 11.40$ eV, were $\approx 250 \pm 20$ meV smaller than the experimental values (Appendix A).

The IE values are consistent with the electron impact values reported by Dibeler *et al.*,⁷² $\text{IE}(\text{HC}_3\text{N}) = 11.6 \pm 0.2$ eV, and by Büchler and Vogt,⁷³ $\text{IE}(\text{HC}_3\text{N}) = 11.6 \pm 0.1$ eV. Our $\text{IE}_{\text{ad}}(\text{HC}_3\text{N})$ and IE_{vert} values agree reasonably well with PES values $\text{IE}_{\text{ad}}(\text{HC}_3\text{N}) = 11.60$ eV⁴⁴ and $\text{IE}_{\text{vert}} = 11.75$ eV reported by Bieri *et al.*⁷⁴ Harland⁶⁰ in a “monochromatic” electron impact study obtained $\text{IE}_{\text{ad}} = 11.56 \pm 0.04$ eV, which is in excellent accord with our TIY value. We note also an early Rydberg series value $\text{IE} = 11.60$ eV.⁷⁵ Calculations by Mendes *et al.* give the difference between $\text{IE}_{\text{vert}} - \text{IE}_{\text{ad}} = 130$ meV,⁵⁰ whereas our CCSD(T) based calculations give 60 meV, in good agreement with our SPES/TIY determined value 70 ± 20 meV (Appendix A).

3. Heat of formation of HC_3N^+

Using the heat of formation of $\Delta_f H(\text{HC}_3\text{N}) = 354$ kJ/mol (3.668 eV), determined by Harland from ion appearance energy measurements in an electron impact study,⁶⁰ our cyanoacetylene ionization energy leads to a value of the heat of formation of the cyanoacetylene ion $\Delta_f H(\text{HC}_3\text{N}^+) = 1471$ kJ/mol (15.241 eV) in good agreement with the value 1469 kJ/mol quoted by Holmes *et al.*⁷⁶ Nevertheless, we consider $\Delta_f H(\text{HC}_3\text{N})$ to be uncertain, as can be seen from the following review of published experimental and theoretical values of $\Delta_f H(\text{HC}_3\text{N})$, detailed here because of the fundamental physico-chemical and cosmochemical importance of having a valid value of the heat of formation of cyanoacetylene and its cation.

Lias *et al.*⁷⁷ give $\Delta_f H(\text{HC}_3\text{N}) = 351$ kJ/mol based on the Harland “experimental” value reported by Knight *et al.*⁷⁸ Okabe and Dibeler⁷⁹ give $\Delta_f H(\text{HC}_3\text{N}) = 355 \pm 5$ kJ/mol based on photoion appearance energies (their value is reported incorrectly as 398 ± 4 kJ/mol by Francisco and Richardson in their study of the heat of formation of cyanoacetylene⁸⁰). A number of theoretical calculations of $\Delta_f H(\text{HC}_3\text{N})$ have been made. A MINDO calculation gave $\Delta_f H(\text{HC}_3\text{N}) = 342.8$ kJ/mol and $\Delta_f H(\text{HC}_3\text{N}^+) = 1404.5$ kJ/mol,⁸¹ whose difference gives $\text{IE}(\text{HC}_3\text{N}) = 11.0$ eV, which is ≈ 600 meV

smaller than our experimental value of the ionization energy. A group-additivity derivation resulted in $\Delta_f H(\text{HC}_3\text{N}) = 380 \text{ kJ/mol}$, with an uncertainty of 20 kJ/mol .⁸² Ochterski *et al.*⁸³ obtain 384.6 kJ/mol via the atomization energy approach, while a Gaussian-4 level calculation of $\Delta_f H(\text{HC}_3\text{N})$, also using atomization energies, gave a different value, 372.0 kJ/mol .⁸⁴ We note also the *ab initio* calculations of Francisco and Richardson at the Gaussian-2 theory level which give $382 \pm 8 \text{ kJ/mol}$, while an isodesmic reaction evaluation gives $379 \pm 8 \text{ kJ/mol}$.⁸⁰ Using an enthalpic shift procedure Golovin and Takhistov⁸⁵ determined $\Delta_f H(\text{HC}_3\text{N}) = 360.7 \text{ kJ/mol}$. Thus reported experimental and calculated values of $\Delta_f H(\text{HC}_3\text{N})$ cover the wide range $342\text{--}382 \text{ kJ/mol}$.

We note that Harland's experimental value $\Delta_f H(\text{HC}_3\text{N}) = 354 \text{ kJ/mol}$, which has been the most "certified" experimental value in data lists, is based on $\Delta_f H(\text{C}_2\text{H})$ and on $\Delta_f H(\text{CN}^+)$. Indeed it depends very critically on the value of $\Delta_f H(\text{CN}^+)$, which is uncertain because of the numerous values of $\text{IE}(\text{CN})$ listed in the NIST compilation.⁸⁶ In this compilation, $\text{IE}(\text{CN})$ has four cited experimental values ranging from $14.03 \pm 0.02 \text{ eV}$ ⁸⁷ to $14.5 \pm 0.2 \text{ eV}$ ⁷² while the $\text{IE}(\text{CN})$ evaluated by Herzberg and Huber is 14.17 eV ⁸⁸ and that given (for unexplicated reasons) by Lias *et al.* in NIST⁸⁶ is 13.598 eV , with $\Delta_f H(\text{CN}^+) = 1750 \pm 4 \text{ kJ/mol}$. More recently, hybrid DFT methods gave calculated values $\text{IE}(\text{CN}) = 13.66$ and 13.88 eV .⁸⁹ The reported experimental and calculated values of $\text{IE}(\text{CN})$ just mentioned thus cover the wide range $13.598\text{--}14.5 \text{ eV}$. We note also that a quite thorough report dating from 1965 elaborates the determination of eight different values of $\text{IE}(\text{CN})$ and recommends the lowest value, $\text{IE}(\text{CN}) = 13.4 \text{ eV}$.⁹⁰ There is therefore an urgent need for a definitive determination of $\text{IE}(\text{CN})$.

The dependence of the heat of formation of HC_3N on $\Delta_f H(\text{C}_2\text{H})$ is difficult to resolve quantitatively since the NIST compilation⁸⁶ gives two widely different values, $\Delta_f H(\text{C}_2\text{H}) = 477 \text{ kJ/mol}$ ⁹⁴ and 556 kJ/mol .⁹⁵ (The book of Holmes *et al.*⁷⁶ lists the following values, which do not appear to be valid: $\Delta_f H(\text{C}_2\text{H}) = 594 \text{ kJ/mol}$ and $\text{IE}(\text{C}_2\text{H}) = 10.64 \text{ eV}$, reported as being from the NIST compilation). Lias *et al.*⁷⁷ give $\Delta_f H(\text{C}_2\text{H}) = 565 \pm 4 \text{ kJ/mol}$ from Ref. 96 and $\text{IE}(\text{C}_2\text{H}) = 11.7 \text{ eV}$. NIST⁸⁶ gives $\text{IE}(\text{C}_2\text{H}) = 11.61 \pm 0.07 \text{ eV}$, basically from the PEPICO study of Norwood and Ng⁹⁷. A more recent value, $\text{IE}(\text{C}_2\text{H}) = 11.645 \pm 0.0014 \text{ eV}$ ⁹⁸ is based on a determination of the threshold energy for formation of C_2H^+ from acetylene, while a recent *ab initio* calculation gave $\text{IE}(\text{C}_2\text{H}) = 11.652 \text{ eV}$.⁹⁹ An early review of the difficulties of determining $\Delta_f H(\text{C}_2\text{H})$ and $\text{IE}(\text{C}_2\text{H})$ occurs in chapter VI of the book of Berkowitz.¹⁰⁰

From the above discussion it is clear that many questions concerning CN and C_2H are still unresolved and require further investigation before conclusive values of $\Delta_f H(\text{HC}_3\text{N})$ and $\Delta_f H(\text{HC}_3\text{N}^+)$ can be obtained.

4. Autoionisation structures

A series of bands are observed in the TIY spectrum of the parent ion between 11.6 eV and the observation limit at 15.6 eV (Figs. 1(b) β and 3 and Table V). These bands must be autoionization features since, as seen in Figure 1(b), they

occur at fixed photon energies and their electron kinetic energies (Fig. 1(a)) do not follow lines of constant slope as in direct ionization. Band assignments are given in Table V and in Figure 3. As mentioned earlier, except in the immediate ionization threshold region, the TIY spectrum is closely similar to, but better resolved than, the VUV absorption spectrum of Ferradaz *et al.*⁶⁸ in the same energy region (Fig. 5). The broad asymmetric features peaking at 11.930 and 12.179 eV in the TIY spectrum (Figs. 5(b) and 5(c) and Table V) correspond to the 11.914 and 12.179 eV features of the SPES spectrum (Fig. 1(b) α , Table III), respectively, assigned to the intense 2^1_0 and 2^2_0 vibronic transitions to the $\text{B}^2\Pi$ state and thus indicate increases in ionization cross-section on excitation of the $\nu_2(\text{C}\equiv\text{N})$ stretching vibration.

There follows a series of much sharper bands in the TIY spectrum, beginning with the feature at 12.446 eV (Fig. 3 and Table V). This feature is assigned to the $n = 3$ member of a Rydberg series R2, quantum defect $\delta = 0.094$. The next strong band, at 12.553 eV is assigned to the $n = 4$, $\delta = 1.0$, member of another Rydberg series, R1, for which we assign the $n = 4\text{--}10$ bands in Table V. Both series, R1 and R2 ($n = 3\text{--}8$ assigned), converge to the $\text{B}^2\Pi \text{O}^0_0$ ion state level at 14.057 eV . We note that an additional member of the R1 series, the $n = 3$ member of the R1 series is observed below the $\text{X}^2\Pi$ ionization limit as a band at $85\,675 \text{ cm}^{-1}$ (10.622 eV) in the absorption spectrum of HC_3N measured by Ferradaz *et al.*⁶⁸ and assigned as $n = 3$, $\delta = 0.99$ by Mendes *et al.*⁵⁰. The latter took $\text{IE}(\text{B}^2\Pi) = 14.03 \text{ eV}$, the HeI PES value of Baker and Turner,⁴⁴ in calculating the quantum defect. With our extensive set of $n = 3\text{--}10$ assigned R1 series of Rydberg bands we obtain a more precise $\text{IE}(\text{B}^2\Pi) = 14.057 \text{ eV}$, as found also with the R2 series limit, in fitting the whole set of Rydberg bands to the formula $T(n) = I - R/(n - \delta)^2$, where $T(n)$ is the Rydberg term value of principal quantum number n , I the ionization energy and R the Rydberg constant. We remark that the R2 series has no precursor in the three-photon REMPI spectra of HC_3N measured by Mendes *et al.*⁵⁰ nor is one reported in the HC_3N absorption spectrum of Ferradaz *et al.*⁶⁸ analysed by Mendes *et al.*⁵⁰

In Table V we also list vibronic components of the R1 series in which progressions of the ν_4 (C–C stretch) vibration are observed. We assign a series $n\sigma^1\Pi 4^1_0$ for $n = 4\text{--}9$, with some 4^2_0 levels also observed ($n = 4, 5, 9$; band overlaps can occur for other values of n). A progression in ν_4 (C–C stretch), bands 4^1_0 and 4^2_0 , has also been listed for the $n = 3$ member in the absorption spectrum⁵⁰ but these $n = 3$ vibronic assignments can be questioned since the reported ν_4 vibronic band intervals, respectively, 1052 and 962 cm^{-1} are considerably greater than our or previously observed values of ν_4 (C–C stretch) for the $\text{B}^2\Pi$ state (Table II). Progressions in ν_4 (C–C stretch) are not observed for the R2 series in the TIY spectrum but they could be present, overlapping some of the R1 series bands. Much higher resolution studies are necessary to clarify the situation.

The allowed Rydberg transitions culminating in the $\text{B}^2\Pi$ ion state at 14.057 eV would be: one s-type and three d-type series:

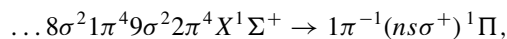


TABLE V. TIY spectrum HC₃N. The pointing errors are estimated to be ± 4 meV.

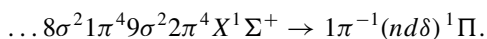
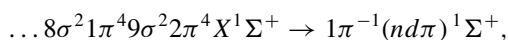
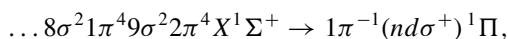
Band No.	Energy (eV)	Energy (cm ⁻¹)	Assignment
1	11.573	93 342	X ² Π O ⁰ ₀ IE _{ad}
1* ^a	11.643 ^a	93 907 ^a	X ² Π O ⁰ ₀ IE _{vert}
2	11.930	96 221	X ² Π 2 ¹ ₀
3	12.179	98 230	X ² Π 2 ² ₀
4	12.298	99 190	
5	12.384	99 883	
6	12.446	100 383	R2 n = 3, δ = 0.094
7	12.508	100 883	
8	12.553	101 246	R1 n = 4, δ = 1.0
9	12.573	101 408	
10	12.621	101 795	
11	12.648	102 012	R1 n = 4, 4 ¹ ₀
12	12.665	102 150	V O ⁰ ₀
13	12.732	102 690	V 6 ¹ ₀
14	12.760	102 912	R1 n = 4, 4 ² ₀
15	12.767	102 972	V 4 ¹ ₀
16	12.805	103 279	V 6 ² ₀
17	12.859	103 714	V 4 ² ₀
18	12.886	103 932	V 3 ¹ ₀
19	12.914	104 158	V 2 ¹ ₀
20	12.997	104 827	
21	13.048	105 239	
22	13.122	105 835	
23	13.173	106 247	R2 n = 4, δ = 0.077
24	13.205	106 505	R1 n = 5, δ = 1.0
25	13.230	106 707	
26	13.280	107 110	R2 n = 4, 4 ¹ ₀
27	13.305	107 311	R1 n = 5, 4 ¹ ₀
28	13.342	107 610	
29	13.405	108 118	R1 n = 5, 4 ² ₀
30	13.444	108 433	
31	13.477	108 699	
32	13.506	108 933	R1 n = 6, δ = 1.03; R2 n = 5, δ = 0.031
33	13.548	109 271	
34	13.604	109 723	R1 n = 6, 4 ¹ ₀
35	13.637	109 989	
36	13.670	110 255	R1 n = 7, δ = 1.07; R2 n = 6, δ = 0.071
37	13.692	110 433	
38	13.745	110 860	
39	13.771	111 070	R1 n = 8, δ = 1.10; R1 n = 7, 4 ¹ ₀ ; R2 n = 7, δ = 0.10
40	13.791	111 231	
41	13.843	111 651	R1 n = 9, δ = 1.03; R2 n = 8, δ = 0.026
42	13.873	111 893	R1 n = 8, 4 ¹ ₀
43	13.892	112 046	R1 n = 10, δ = 0.92
44	13.932	112 369	R1 n = 9, 4 ¹ ₀
45	13.967	112 651	
46	14.034	113 191	R1 n = 9, 4 ² ₀
47	14.304	115 369	... ^b
48	14.712	118 660	
49	14.862	119 869	
50	14.917	120 313	
51	15.023	121 168	
52	15.081	121 636	
53	15.117	121 926	
54	15.141	122 120	
55	15.191	122 523	
56	15.238	122 902	
57	15.320	123 563	
58	15.375	124 007	
59	15.473	124 797	

TABLE V. (Continued).

Band No.	Energy (eV)	Energy (cm ⁻¹)	Assignment
60	15.515	125 136	
61	15.546	125 386	
62	15.592	125 757	

^aFrom SPES spectrum (Sec. V A 1 and Table III).

^bBands Nos. 47–62 are possibly features of Rydberg series converging to the C²Σ⁺ ion state at 17.62 eV, Sec. V C 1.



Our assigned R1 Rydberg series $n = 4$ –10, have quantum defects $\delta = 0.92$ –1.10, while for the R2 Rydberg series $n = 3$ –8, $\delta = 0.03$ –0.10 (Table V). The R2 series bands for $n > 4$ overlap those of the R1 series. The R1 series most probably corresponds to states derived from ns electrons, and the R2 from nd electrons, the latter giving rise to transitions such as $(nd\pi)^1\Sigma^+ \leftarrow ^1\Sigma^+$ or $(nd\delta)^1\Pi \leftarrow ^1\Sigma^+$ which are expected to have quantum defects of the order of magnitude observed for the R2 series.¹⁰¹ We note that on the basis of the united atom model,⁹³ with argon considered as the united atom valid for HC₃N, the strongest Rydberg transitions in cyanoacetylene are expected to involve only ns and nd Rydberg series.⁵⁰

5. Photoelectron spectra

It is of interest to analyse the relaxation pathways by measuring the electron kinetic energy. Figure 6 displays KE projections for the photon energies corresponding to selected Rydberg (Fig. 6(a)) and valence (Fig. 6(b)) bands as well as some non-assigned but possible Rydberg band features (Fig. 6(c)). The spectra at specific band excitation energies will contain two components, a background component due to direct ionization and a resonance component due to autoionization. In the latter case the ionizing transition is indirect, in that it now occurs from a superexcited neutral state lying above the ionization energy.

In Fig. 6(a) the photoelectron spectra associated with Rydberg Band Nos. 6, 8, 23, 24, 32, and 36 in Table V (TIY spectrum) correspond to increasing values of the principal quantum number n of the two series R1 and R2. The bands become broader as n increases, which may indicate an evolving decrease of the Rydberg state lifetimes with increasing principal quantum number. The valence state spectra, Bands Nos. 12, 13, 15, 18 and 19 (Fig. 6(b) and Table V) discussed in Sec. V E, are little changed with increasing internal energy, indicating constant lifetimes on the scale of our energy resolution, and thus a set of similar vibronic couplings to the ionization continuum.

Fig. 6(c) gives the photoelectron spectra associated with Bands 47, 49, 55, 58, 61, and 62 (Table V) which are considered as possible Rydberg bands converging to the C²Σ⁺ state of the ion (see below, Sec. C 1). Here too there are increas-

ing widths of the photoelectron bands with increasing energy, most clearly seen in the 13–15 eV binding energy region.

C. Further Rydberg transitions

In this section we discuss some aspects of other Rydberg transitions in cyanoacetylene. We note first of all the absence of Rydberg bands converging to A²Σ⁺ state in the

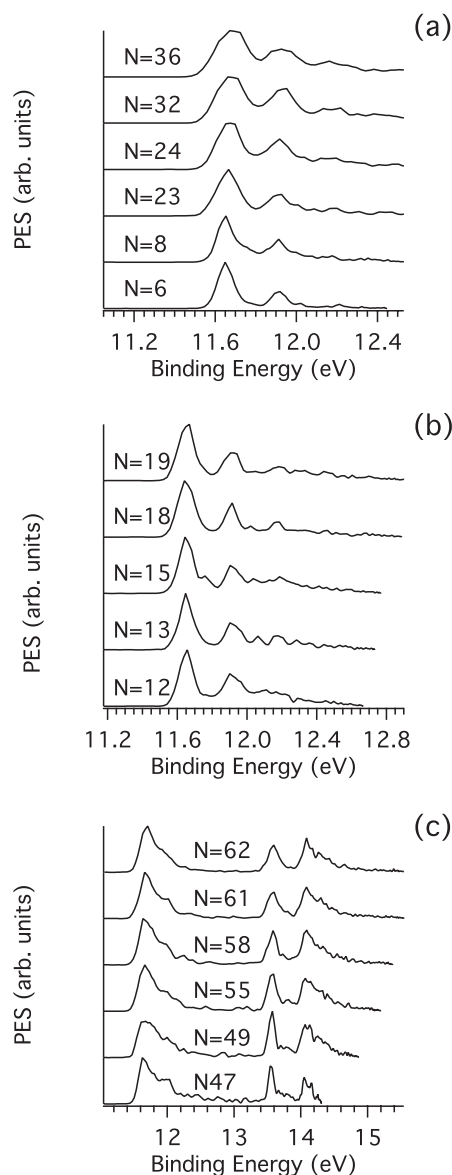


FIG. 6. Cyanoacetylene: photoelectron spectra at different fixed photon energies corresponding to the band numbers (N) referenced in Table V. See text for description.

TIY spectrum and none have been reported in the absorption spectra of HC₃N.^{50,79,102} We have previously mentioned the absence of $A^2\Sigma^+ \leftarrow X^2\Pi$ HC₃N⁺ absorption features in the Ne matrix work.⁵⁹ However, we think it would be worthwhile re-investigating parts of the absorption spectra assigned by Mendes *et al.*⁵⁰ in order to verify the presence or absence of Rydberg bands converging to $A^2\Sigma^+$ state of HC₃N.

Two other energy regions of the HC₃N TIY spectra merit the following discussion of Rydberg series aspects.

1. Rydberg bands converging to the $C^2\Sigma^+$ state?

There are features in the 14.7–15.6 eV region of the TIY spectrum, in particular the six bands Nos. 47, 49, 55, 58, 61, and 62 (Figs. 5(b) and 5(c) and Table V) at 14.304, 14.862, 15.191, 15.375, 15.546, and 15.592 eV, respectively, which are possibly Rydberg vibronic bands converging to the $C^2\Sigma^+$ ion state whose origin is reported to be at 17.62 eV⁴⁴ (other possible origin bands are discussed in Appendix B). The He I⁴⁴ and He II⁴⁵ PES spectra exhibit a series of vibronic bands, maximum intensity at 18.2 ± 0.1 eV, extending from 17.62 eV to the beginning of a continuum at about 18.6 eV. The average interval of these bands is of the order of 1320 cm^{-1} according to Baker and Turner⁴⁴ (see also the discussion in Appendix B). They assigned this interval to the ν_1 (C–H) vibration whose frequency is greatly diminished with respect to the neutral species (Table II).

We suggest that the 15.2 ± 0.4 eV TIY region could correspond to $n = 3$ members of Rydberg series converging to the $C^2\Sigma^+$ ion state. In this case the TIY spectrum should exhibit vibrational structure similar to that of the $C^2\Sigma^+$ ($8\sigma \rightarrow 2\pi$) state PES band. To verify this requires more extensive TIY spectra and higher resolution PES spectra than available at present.

2. Rydberg bands converging to the $X^2\Pi 2^1$ vibronic level

Here we consider some aspects of Rydberg series converging to vibronic components of the $X^2\Pi$ ion state. For this we have re-examined the photoionization yield curves for HC₃N in the 11.59–11.98 eV region measured with a hydrogen discharge VUV light source by Okabe and Dibeler.⁷⁹ Their parent ion yield spectrum is much better resolved than our TIY spectrum in this energy region. Okabe and Dibeler reported a series of features corresponding to $n = 8$ –14 and $n = 8$ –15 members of two Rydberg series, converging to the 2^1 vibrational level of the $X^2\Pi$ state, with quantum defects $\delta = 0.95$ and 0.55 , respectively, and an $X^2\Pi 2^1$ Rydberg limit of $96\,073 \text{ cm}^{-1}$ (11.912 eV). We note that this limit agrees well with our $X^2\Pi 2^1$ SPES band at 11.914 eV (Table III). Individual photoionization yield peak energies were not listed by Okabe and Dibeler.

We enlarged Fig. 4 of the Okabe and Dibeler PIY curve⁷⁹ and measured the energies of 20 peaks between 11.59 eV and 12 eV. The values reported in Table VI should be considered as subject to measuring errors of the order of 5 meV. These 20 features include the Rydberg bands, assigned by

Okabe and Dibeler, which converge to the ion ground state $X^2\Pi 2^1_0$ vibronic level at 11.914 eV. There are also some bands in the 11.88–11.98 eV region that can be considered to form part of unanalysed Rydberg series converging to the $X^2\Pi 2^2_0$ vibronic level at 12.179 eV as limit. The separation, for example, between the bands at 11.652 and 11.924 eV is 2187 cm^{-1} , which is compatible with a ν_2 vibrational frequency in the $X^2\Pi$ ion state (Table II). In order to see whether the Okabe/Dibeler bands listed in Table VI are also present in our much less well resolved TIY spectrum we noted the successive intensity maxima in the TIY ion counts as a function of excitation energy in the energy range 11.64–11.98 eV. The energies of these maxima are also listed in Table VI. There is reasonable agreement, generally to within ± 4 meV, between the two sets of energies, taking into account the manner of measurement in both cases and noting that the measurement interval of Okabe and Dibeler in the 12 eV region was 11 meV, whereas our TIY measurement interval was 4 meV. The largest difference, 9 meV, between the two measurement sets of Table VI, concerns the unassigned broadest feature in these series of bands, peaking at 11.924 eV on a sharply rising curve in the Okabe/Dibeler spectrum. Using the measured values we were unable to make satisfactory consistent quantum defect fits to the two Rydberg series equations published by Okabe and Dibeler.⁷⁹ This illustrates the very great sensitivity of the quantum defect in the Rydberg formula to the energies of bands corresponding to high values of the principal quantum number n . In addition to the measurement limitations and uncertainties, part of the fitting difficulty could also be due to irregularities in the Rydberg levels due to electronic and vibronic interactions. We mention that Mendes *et al.*⁵⁰ have assigned some of the absorption bands of Ferradaz *et al.*⁶⁸ to lower members, $n = 3$ –5, of three Rydberg series converging on the $X^2\Pi 2^1_0$ vibronic level with quantum yields, respectively, ≈ 1.0 , ≈ 0.41 , and -0.06 . We recall that Connors *et al.* reported two Rydberg series converging to $X^2\Pi 0^0_0$ with $\delta = 1.0$ and 0.40 , respectively.¹⁰² The quantum defect values of Mendes *et al.* and of Connors *et al.* do not allow us to make satisfactory Rydberg series fits for the Okabe/Dibeler derived data of Table VI.

D. H-loss channels

Although our calculation of the vertical excitation energy for the $C^2\Sigma^+$ state is in excellent agreement with the HeI PES study of Baker and Turner⁴⁴ (see Appendix A), our calculation of the $C^2\Sigma^+$ state ν_1 (C–H) frequency (Table II) results in a value, 3347 cm^{-1} , far from the $\nu_1 \approx 1320 \text{ cm}^{-1}$ reported in the same study. We note, however, that a close examination of this PES band (expanded Fig. 11 of Ref. 44) indicates that the initial peak intervals $\Delta\nu$ are of the order of 1600 cm^{-1} up to the band maximum at 18.2 ± 0.1 eV and become much smaller, $\Delta\nu \leq 900 \text{ cm}^{-1}$, above 18.4 eV.

A more refined theoretical calculation, which explores the potential energy surface leading to C–H dissociation was required in order to clarify this question. This was carried out by the methods described in Sec. III, not only for the $C^2\Sigma^+$ state but also for the ground $X^2\Pi$ and the first two electronic excited states of the ion, $A^2\Sigma^+$ and $B^2\Pi$. In this section we

TABLE VI. HC₃N : (a) Measurements of PIY from fig. 4 of Okabe and Dibeler⁷⁹ compared with (b) our TIY measurements.

Band No.	λ (Å) (a)	ν (cm ⁻¹) (a)	E (eV) (a)	Our TIY (b)	(a) – (b) meV	Assignment ⁷⁹
1	1064.02	93 983	11.652	11.649	+3	R _a n = 8 ?
2	1062.98	94 075	11.664	11.669	-5	R _b n = 8
3	1060.17	94 324	11.694	11.697	-3	R _a n = 9
4	1058.91	94 436	11.709	11.709	0	
5	1057.81	94 535	11.721	11.725	-4	R _b n = 9
6	1056.36	94 665	11.737	11.741	-4	R _a n = 10
7	1055.10	94 778	11.751	11.753	-2	
8	1053.62	94 911	11.767	11.769	-2	R _b n = 10
9	1052.36	95 024	11.782	11.785	-3	R _a n = 11
10	1051.45	95 107	11.792	11.793	-1	R _b n = 11
11	1049.94	95 244	11.809	11.805	+4	R _b n = 12
12	1048.36	95 387	11.827	11.829	-2	R _a n = 13 ; R _b n = 13
13	1047.57	95 459	11.835		?	R _a n = 14 ; R _b n = 14
14	1046.82	95 528	11.844	11.845	-1	R _a n = 15 ; R _b n = 15
15	1043.26	95 853	11.884	11.881	+3	
16	1041.94	95 975	11.899	11.899	0	
17	1039.83	96 170	11.924	11.933	-9	
18	1038.28	96 313	11.941	11.945	-4	
19	1037.02	96 430	11.956	11.957	-1	
20	1035.89	96 535	11.969	11.973	-4	

discuss the results that provide new information on the H-loss dissociation channels for these states. The results concerning the C²Σ⁺ state ν_1 (C–H) frequency are presented in Appendix B.

Figure 7(a) shows the potential energy profile for the ground and three excited electronic states of the cyanoacetylene ion along the C–H elongation channel between $r(\text{C–H}) = 0.6$ and 3.0 Å. The calculations were carried out up to $r(\text{C–H}) = 9$ Å and 10 Å which were at the dissociation limits since there were no differences in the state energies at these two internuclear distances. The calculated C–H dissociation limits were respectively 5.82 eV (X²Π), 7.16 eV (A²Σ⁺), 6.98 eV (B²Π), and 7.33 eV (C²Σ⁺).

The calculated C–H dissociation energy for the X²Π state, 5.82 eV, is in reasonable agreement with the experimental value $D(\text{C–H}) = 6.22$ eV of Harland⁶⁰ who observed $AE(\text{C}_3\text{N}^+) = 17.78 \pm 0.08$ eV in an electron impact experiment on cyanoacetylene. It is also of the same order of magnitude as the corresponding calculated value (there is no direct experimental value) for neutral linear cyanoacetylene. Some representative calculated values of the neutral molecule C–H dissociation energy are 5.70 ± 0.08 eV¹⁰³ and 5.99 ± 0.09 eV⁸⁰ but these are both based on a calculation of $\Delta_f H(\text{C}_3\text{N})$, for which a wide variety of values have been reported. More relevant is a recent calculation, by a scaled hypersphere search method, of the potential energy surfaces of dissociation channels for the linear and cyclic isomers of HC₃N.¹⁰⁴ All dissociation channels of the isomers were found to correspond to direct decomposition without transition states. For the linear form HCCCN the hydrogen-loss channel dissociation energy was 5.518 eV whereas for four different cyclic isomers the $D(\text{C–H})$ values were in the range 2.3 – 3.5 eV.

The C–H dissociation channel profiles of the A²Σ⁺ and B²Π states of the ion the lead to dissociation energies whose

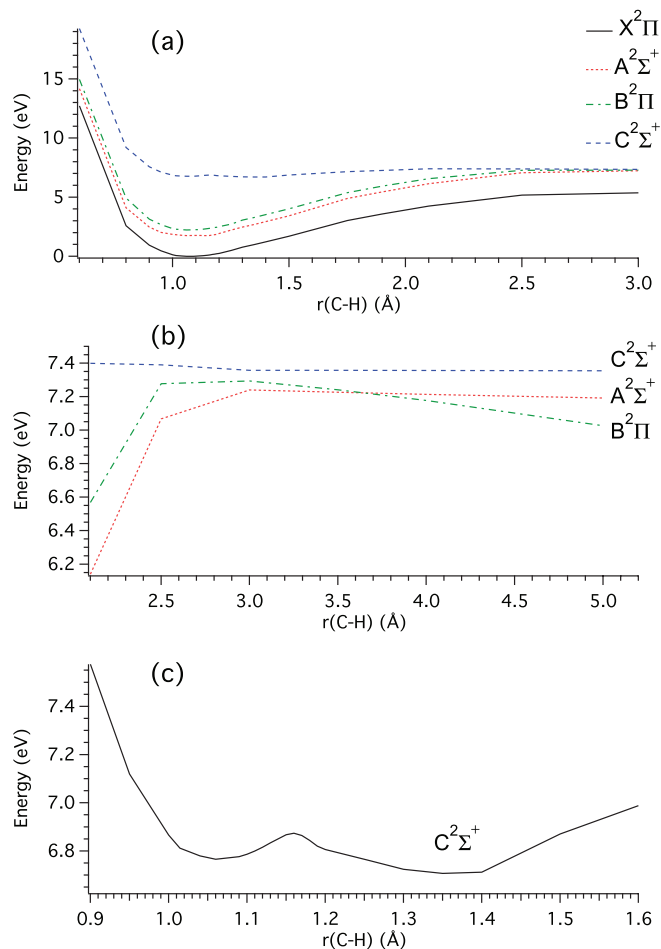


FIG. 7. (a) Calculated potential energy profiles of the C–H dissociation channel of the X²Π, A²Σ⁺, B²Π, and C²Σ⁺ electronic states of HC₃N⁺ (For calculation method see Sec. III). (b) Expanded profiles for the A²Σ⁺, B²Π, and C²Σ⁺ electronic states between $r(\text{C–H}) = 2.3$ and 5 Å. (c) Expanded profile for the C²Σ⁺ state between $r(\text{C–H}) = 0.9$ and 1.43 Å.

TABLE VII. C_3N^+ electronic states and combination with $H(^2S_g)$ to form HC_3N^+ electronic states.

C_3N^+ electronic state	Linear symmetry ($C_{\infty v}$)	Energy ^a (meV)	Linear HC_3N^+ electronic states resulting from $C_3N^+ + H(^2S_g) \rightarrow HC_3N^+$
$^3A (C_1)$ quasi-linear CCCN ⁺	$^3\Pi$	0.0	$X^2\Pi, ^4\Pi$
$^3\Sigma^- (C_{\infty v})$ linear CCCN ⁺	$^3\Sigma^-$	8.7	$^2\Sigma, ^4\Sigma$ (probably non-stable dissociative states correlating with very highly excited HC_3N^+ electronic states)
$^3A (C_1)$ quasi-linear CCNC ⁺	$^3\Pi$	429	$B^2\Pi, ^4\Pi$
$^1A'(C_s)$ quasi-linear CCCN ⁺	$^1\Sigma^+$	598	$A^2\Sigma^+$
$^1A'(C_s)$ quasi-linear CCNC ⁺	$^1\Sigma^+$	945	$C^2\Sigma$

^aEnergies from the supplementary material in Wang *et al.*¹⁰⁵

magnitudes, of the order of several eV, respectively, 5.38 and 4.78 eV, are similar to that of the $X^2\Pi$ state and would appear to correspond to simple bond rupture in each case. However, for the $C^2\Sigma^+$ state the calculated dissociation limit corresponds to a C–H dissociation energy of 560 meV. The ground state of HC_3N^+ would dissociate into unexcited linear $C_3N^+ + H$, while the dissociation limits of the excited electronic states could correspond to formation of an electronically excited C_3N^+ fragment ion and a neutral H atom.

The various product possibilities and the relative energy differences between them are presented in Table VII, which we derived from application of Wigner-Witmer correlation schemes⁹³ and the energies of quasi-linear electronic states of the C_3N^+ ion, whether as CCCN⁺ or CCNC⁺, calculated by Wang *et al.*¹⁰⁵ at the B3LYP/6-311 + G(3df) level of theory, with relative energies and electronic states determined at the CCSD(T)/aug-cc-pVTZ level. The data in Table VII, in which we consider the combining electronic states of C_3N^+ as having $C_{\infty v}$ symmetry, predict that the C–H dissociation limit of the $A^2\Sigma^+$ state lies 169 meV above that of the $B^2\Pi$ state. This agrees with the order given by the results of our C–H dissociation potential energy profile calculations which predict a dissociation limit energy difference of 180 meV. Figure 7(b) illustrates the calculated crossover of the $A^2\Sigma^+$ and $B^2\Pi$ states at about $r(C-H) = 3.6$ Å. Table VII also predicts the dissociation limit of the $C^2\Sigma^+$ state to lie 347 meV above that of the $A^2\Sigma^+$ state, in reasonable agreement with the value 516 meV of our calculated difference of dissociation limits between these two states.

We note that in the electron impact experiment of Harland⁶⁰ a second onset (sharp rise) was observed at 18.64 ± 0.08 eV in the C_3N^+ yield curve, i.e., 860 ± 160 meV above the first dissociation limit. This is of the same order of magnitude as the difference between the calculated dissociation limits of the ground state $A^2\Pi$ and the $B^2\Pi$ state, 1160 meV. We remark that the experimental set-up of Harland would allow for a metastable excited state C_3N^+ to be recorded.

Up to now we have considered the C_3N^+ product to be linear or quasi-linear. However, another possibility is that on dissociation from the electronically excited states of the cyanoacetylene ion the C_3N^+ ion is formed in a cyclic isomeric form. Harland and Maclagan¹⁰⁶ also carried out *ab ini-*

tio calculations of the relative energies for various structures and electronic excited states of the C_3N^+ ion. Although they tend to prefer formation of the cyclic isomer, the results, as well as those of calculations on the structures and energies of C_3N^+ isomers by Ding *et al.*^{107,108} do not eliminate the suggestion of formation of an excited state of a linear or quasi-linear C_3N^+ ion.

The recent calculation on C_3N^+ structures and electronic state energies by Wang *et al.*¹⁰⁵ discussed above, indicated that for the linear isomer of C_3N^+ , a quasi-linear excited singlet state should exist at 598 meV above a triplet ground state (Table VII), whereas for two cyclic isomers their ground electronic states should lie at, respectively, 1105 meV and 1534 meV above ground state of the linear isomer. As dissociation products, a linear C_3N^+ excited electronic state and an unexcited cyclic C_3N^+ isomer are thus each compatible with the ion yield experimental⁶⁰ data. In this respect we mention also that Selected-Ion Flow Tube (SIFT) studies of the reactions of C_3N^+ with a number of different molecules have provided evidence for the existence of one major ($\geq 90\%$ in some cases) and one minor ($\leq 10\%$) different reactive forms of C_3N^+ .^{78,109} This is based on the observation of differences in ion/molecule reaction rate coefficients for the two C_3N^+ species. Petrie *et al.*¹⁰⁹ consider that the less reactive form could not be an excited form of the major (linear) component, arguing that electronic excitation energy should also promote its reactivity. However, we consider that this argument loses its absoluteness in the present case where the excited states of quasi-linear C_3N^+ in the relevant energy region are singlet states and so have a different spin multiplicity from that of the ground state.

E. Valence shell transitions

There are a number of features in the TIY spectrum, in particular in the 12.6–13.1 eV region that have not been assigned to Rydberg series (Fig. 3 and Table V). Some of these features can be considered as arising from valence shell transitions. Information on such transitions in cyanoacetylene can be obtained from Connors *et al.*¹⁰² who carried out molecular orbital calculations of valence shell transitions in the 31 800–106 000 cm^{-1} (3.94–13.14 eV) region, using the CNDO/2 method. In the energy region above the first IE there are

calculated to be 3 dipole transitions of interest, two of which are to excited $^1\Sigma^+$ states and one to a $^1\Pi$ state:

- (i) $99\,200\text{ cm}^{-1}$ (12.30 eV), $f = 0.007$, $^1\Sigma^+$;
- (ii) $104\,400\text{ cm}^{-1}$ (12.94 eV), $f = 0.008$, $^1\Pi$;
- (iii) $106\,000\text{ cm}^{-1}$ (13.14 eV), $f = 1.4$, $^1\Sigma^+$.

These valence shell transitions are possibly responsible for at least some of the $m/z = 51$ TIY bands we see in the 12.6–13.1 eV region and that have not been assigned to Rydberg states. Some provisional assignments to vibrational components of the expected strong $^1\Sigma^+ \leftarrow \Sigma^+$ valence transition, with the 12.665 eV band as O^0_0 origin band, are given in Table V and Fig. 3, where they are indicated as V bands. The vibrational components include several modes, whose vibrational frequencies, $\nu_2 = 2008\text{ cm}^{-1}$, $\nu_3 = 1782\text{ cm}^{-1}$, $\nu_4 = 822\text{ cm}^{-1}$ and $\nu_6 = 540\text{ cm}^{-1}$ are similar to those observed in the $B^2\Pi$ state of the ion, taking into account measurement error bars. We note also that practically all of the TIY features listed in Table V have their counterparts in the VUV absorption spectrum (Fig. 5).

Further work is required in order to deepen our analysis of the autoionizing features in the TIY spectra. In particular, more sophisticated calculations of the high energy valence transitions of HC_3N are necessary, as well as higher resolution absorption spectra of cyanoacetylene in the 11–15 eV region which would help to sort out features arising from autoionization and direct ionization and enable us to clarify and confirm the Rydberg and valence transitions.

F. Some Astrophysical implications

Possible astrophysical applications of our results presented in Secs. V A–V E concern mainly the spectroscopic and thermochemical data, the photophysical excitation mechanisms, the determination of ionization cross-sections, and their relation to absorption phenomena. These data can be crucial for use in cosmochemical reaction schemes applied to different astrophysical contexts, planetary (Titan), circumstellar and interstellar as well as for the interpretation of cometary observations.

The ionization quantum yield Φ_i of a molecular species and its variation at specific excitation energies is a particularly important property to measure that needs to be taken into account in astrophysical chemical reaction schemes. In Sec. V B 1 b we have used a rule of thumb⁷⁹ to estimate Φ_i values of cyanoacetylene at specific photon excitation energies. We remark that the cyanoacetylene cation is very stable under VUV irradiation. The first dissociative ionization process occurs at about 18 eV,⁶⁰ i.e., at over 6 eV above the ionization energy, and about 4.4 eV above the astrophysical HI region energy upper limit, 13.6 eV. Thus if HC_3N is formed in HI regions of the interstellar medium (ISM) it should have no tendency to undergo dissociative ionization in these regions.

VI. CONCLUSION

Cyanoacetylene and its cation are important species whose presence in astrophysical sites is expected or observed.

In particular these species play a role in the atmosphere of Titan where they are subject to charged particle and photon irradiation. The effects of VUV radiation on cyanoacetylene were studied using synchrotron radiation combined with electron/ion coincidence techniques over the excitation range 10–15.6 eV. A detailed analysis of the SPES spectrum in the 11.0–15.5 eV excitation energy region was carried out. The $X^2\Pi$ ground state of the cation shows an onset at $IE_{\text{ad}} = 11.573\text{ eV}$ in the TIY spectrum, in reasonable agreement with previous PES and electron impact values. The heat of formation of the cyanoacetylene cation is uncertain, due to ambiguous values of the heat of formation of neutral HC_3N . There are vibrational components in the SPES spectra in the 11.6–12.2 eV $X^2\Pi$ region which involve the ν_1 (C–H), ν_2 ($\text{N}\equiv\text{C}$), ν_3 ($\text{C}\equiv\text{C}$), and ν_6 (bend) frequencies.

Analysis of SPES features in the 13.5–14.0 eV spectral region provides new aspects, including refined ionization energies and new assignments of vibrational components to the excited $A^2\Sigma^+$ state, whose origin band is at 13.557 eV. Excitation of the ν_1 (C–H), ν_2 ($\text{N}\equiv\text{C}$), ν_3 ($\text{C}\equiv\text{C}$), ν_4 (C–C), and ν_6 (bend) vibrations is observed. The possible existence of vibronic interactions involving the $A^2\Sigma^+$ state is invoked to explain spectral irregularities. The $B^2\Pi$ excited state at 14.053 eV exhibits vibrational components in which ν_1 (C–H), ν_2 ($\text{N}\equiv\text{C}$), ν_3 ($\text{C}\equiv\text{C}$), and ν_4 (C–C) are excited. We also discuss information on three bending vibrations ν_5 , ν_6 , and ν_7 in the $B^2\Pi$ ion state obtained, in part, by re-analysis of published Ne matrix absorption spectra of the cyanoacetylene cation.

A considerable number of autoionization features is observed in the Total Ion Yield spectrum of the parent ion between 11.6 eV and the 15.6 eV observation limit. The total photoionization cross-section has been measured over this photon energy range and the problem of appropriate cross-section calibration has been discussed. The structured autoionization features bear a close resemblance to the VUV absorption spectrum of cyanoacetylene in this spectral region. We have assigned for the first time many of these TIY features to members of two Rydberg series, ns and nd respectively, which converge to the $B^2\Pi O^0_0$ ion state level at 14.057 eV. Vibronic components in ν_4 (C–C) are also observed and fully analysed. Some aspects of the autoionization processes were monitored via photoelectron kinetic energy spectra measured at a number of specific photon excitation energies.

Some further aspects of Rydberg series in cyanoacetylene are also discussed, in particular very weak features in the TIY spectrum that are assignable to Rydberg series converging to the 2^1 vibrational level of $X^2\Pi$, and clearly observed bands in the 14.7–15.6 eV region which are possibly Rydberg vibronic bands converging to the $C^2\Sigma^+$ ion state at 17.62 eV. Consideration of the vibrational structure of the $C^2\Sigma^+$ state has led us to investigate theoretical aspects of the H-loss dissociation channels of the ground and three excited electronic states of the ion.

We conclude with a short discussion of our work and results in the context of implications for astrophysics. The possible astrophysical applications concern mainly the stability of cyanoacetylene under VUV irradiation, the spectroscopic aspects, in particular the extensive Rydberg series,

photophysical excitation mechanisms, the determination of ionization cross-sections, and their relation to absorption phenomena, as well as to the determination of ionization quantum yields as a function of excitation energy which is an important factor in many cosmochemical reaction schemes. Aspects of the theoretical calculations that have been useful in our study are presented in two appendices.

ACKNOWLEDGMENTS

We are indebted to the general staff of SOLEIL for running the synchrotron radiation facility, and in particular to J.-F.Gil, for technical help on the DESIRS beamline. M.S. acknowledges financial support by the French National program Physique et Chimie du Milieu Interstellaire (PCMI). We thank Jean-Claude Guillemin, Université de Rennes, for a generous gift of cyanoacetylene.

APPENDIX A: CALCULATED BONDLNGTHS, ENERGIES AND VIBRATIONAL FREQUENCIES OF HC_3N^+ ELECTRONIC STATES

1. Bondlengths in HC_3N and HC_3N^+ electronic states

We comment on Table I that groups experimental and theoretical geometrical parameters of neutral and cationic cyanoacetylene. For the $X^1\Sigma^+$ ground state of neutral HC_3N , we note that PBE0/AVTZ bondlengths are very close to CCSD(T)/AVTZ values, with a difference less than 1%, and that both methods reproduce very well experimental geometrical parameters, with a difference less than 0.7%. Compared to previous theoretical calculations we note that the geometrical parameters of the HC_3N $X^1\Sigma^+$ state are in good agreement with previous *ab initio*,^{50,51} and DFT⁵² calculations.

For the HC_3N^+ cation, no experimental measurements of bondlengths have been reported in the literature. Our PBE0/AVTZ and CCSD(T)/AVTZ calculation values for the ion ground state $X^2\Pi$ exhibit differences between 0.5% and 2% and we remark that the PBE0 results are closer than those of the CCSD(T) calculations to the values given by previous calculations.^{50,55,56} A comparison of PBE0 geometrical parameters with CASPT2/AVTZ values reported in Ref. 50 for both the A and B states of the cation shows good agreement, with a difference of less than 2% for the $A^2\Sigma^+$ state and 4% for $B^2\Pi$ state. This increases the level of confidence on our PBE0/AVTZ calculations for the $C^2\Sigma^+$ state of the cation HC_3N^+ .

2. Vibrational frequencies in HC_3N and HC_3N^+ electronic states

In this paragraph we comment on Table II, which presents vibrational frequencies of the neutral cyanoacetylene ground state and the four lowest lying electronic states of HC_3N^+ obtained by various experimental and theoretical methods. For the ground state of the cation we performed theoretical calculations of harmonic frequencies with both CCSD(T)/AVTZ and PBE0/AVTZ methods. We note that both methods overestimate vibrational frequencies by about

TABLE VIII. Adiabatic and vertical lowest ionization energy of cyanoacetylene (eV).

Method	DFT/PBE0	CCSD(T)	Experimental (present study)
Basis	AVTZ	AVTZ	
Adiabatic ionization energy	11.30	11.57	11.573
Vertical ionization energy	11.40	11.63	11.643

2%–8% compared to experimental values, which is in line with usual comparisons between harmonic and anharmonic molecular vibrational frequency values. The frequencies obtained by our CCSD(T) calculations are close to those given by PBE0 methods (differences of no more than 1%) as well as to the DFT calculation values reported by Lee⁵⁵ and by Zhang *et al.*⁵⁶ We used the less time-consuming PBE0/AVTZ method in vibrational mode frequency calculations for the A, B, and C excited electronic states of the cation. Our calculations represent the first theoretical determinations of the vibrational frequencies of these excited electronic states of the cyanoacetylene cation. The PBE0/AVTZ calculations reproduce reasonably well the known experimental vibrational frequencies for these states. Differences between experimental and calculated values are partially due to the fact that the calculations are of harmonic frequencies but they can also imply doubtful vibrational assignments or the existence of particular potential energy surfaces such as in the case of $\nu_1(\text{C-H})$ in the $C^2\Sigma^+$ state, discussed in Sec. V D and Appendix B.

3. Ionization energy calculations

The ionization energy calculations were carried out by two different methods, DFT/PBE0 and CCSD(T), with the AVTZ basis set. The vertical ionization energies (IE_{vert}) values were calculated as the difference between the energies of the neutral and the cation, both taken at the equilibrium geometry of the neutral. The adiabatic ionization energies (IE_{ad}) values were deduced as the energy difference between the neutral and the ion at their respective equilibrium structures, and including zero point vibrational energy (ZPE) corrections. Agreement with the experimental lowest ionization energies IE_{ad} and IE_{vert} is particularly good for the CCSD(T) calculations (Table VIII).

Calculations of the vertical excitation energies relative to the $X^2\Pi$ state of the ion were carried out by the CASSF/AVTZ and MRCI/AVTZ methods. The calculated values did not include Zero Point Energy contributions but are in good or reasonable agreement with experimental values (Table IX). We note that the MRCI/AVTZ calculations are in better agreement than the CASSF/AVTZ values with experimental values for the $A^2\Sigma$ state. We remark also that our calculation values of the vertical ionization energy of the $C^2\Sigma^+$ state relative to the $X^2\Pi$ state of the ion, 6.77 eV (CASSF/AVT) and 6.72 eV (MRCI/AVT) are in excellent agreement with the experimental value, 6.56 ± 0.10 eV derived as the difference in energy between the

TABLE IX. Dominant electron configurations and vertical ionization energy (in eV) of electronic states of HCCCN⁺. Vertical ionization energies are relative to the minimum of the X²Π ground state.

Electronic state	Dominant electron configuration	CASSF/AVTZ	MRCI/AVTZ	Experiment
X ² Π	(1σ) ² (2σ) ² (3σ) ² (4σ) ² (5σ) ² (6σ) ² (7σ) ² (8σ) ² (1π) ⁴ (9σ) ² (2π) ³	0	0	0
A ² Σ ⁺	(1σ) ² (2σ) ² (3σ) ² (4σ) ² (5σ) ² (6σ) ² (7σ) ² (8σ) ² (1π) ⁴ (9σ) ¹ (2π) ⁴	1.78	1.93	1.914 ^a
B ² Π	(1σ) ² (2σ) ² (3σ) ² (4σ) ² (5σ) ² (6σ) ² (7σ) ² (8σ) ² (1π) ³ (9σ) ² (2π) ⁴	2.20	2.68	2.41 ^a
C ² Σ ⁺	(1σ) ² (2σ) ² (3σ) ² (4σ) ² (5σ) ² (6σ) ² (7σ) ² (8σ) ¹ (1π) ⁴ (9σ) ² (2π) ⁴	6.77	6.72	6.56 ± 0.10 ^{a,b}

^aPresent study.^bFrom Ref. 44.

C²Σ⁺ state maximum at 18.2 ± 0.1 eV in the He I PES (see Sec. V C 1) and our IE_{vert} = 11.643 eV.

APPENDIX B: REMARKS ON THE ORIGIN BAND AND ON THE ν₁(C–H) VIBRATION OF THE C²Σ⁺ STATE IN THE He I PHOTOELECTRON SPECTRUM OF CYANOACETYLENE

The origin band of the C²Σ⁺ state in the He I photoelectron spectrum of cyanoacetylene was reported by Baker and Turner⁴⁴ to be at 17.62 eV. If this is considered as IE(C²Σ⁺), the experimental appearance energy AE (C₃N⁺) = 17.78 ± 0.08 eV of Harland⁶⁰ for the dissociative ionization reaction HC₃N + hν = > C₃N⁺ + H would then correspond to a C–H dissociation energy of 160 meV in the C²Σ⁺ state. This is rather less than the 560 meV we calculate (Sec. V D).

Examination of a magnified version of the 16–19 eV portion of the He I PES of Baker and Turner (Fig. 11 of Ref. 44) showed that there are at least four bands in the C²Σ⁺ state threshold region that could possibly be assigned as the O⁰₀ band of the C²Σ⁺ state. From the expanded figure we measured bands at 17.15, 17.28, 17.46, and 17.59 eV. This last certainly corresponds to the 17.62 eV band assigned by Baker and Turner. These four bands, as possible C²Σ⁺ state O⁰₀ features, would lead to H-loss dissociation energies in this state of, respectively, 630, 500, 320, and 190 meV, to be compared with the 560 meV from our calculated potential energy profile for the dissociation channel. This suggests that the 17.15 or 17.28 eV PES band is the C²Σ⁺ state O⁰₀ band.

Concerning the reported ≈1320 cm⁻¹ vibrational frequency in the C²Σ⁺ state we first note that a close examination of the C²Σ⁺ PES band (expanded Fig. 11 of Ref. 44) indicates that the initial peak intervals are of the order of 1600 cm⁻¹ up to the band maximum at 18.2 ± 0.1 eV and become much smaller, ≤900 cm⁻¹ above 18.4 eV. We now consider Figure 7(c) which is an expanded version of the potential energy profile between r(C–H) = 0.9 and 1.43 Å. It shows evidence of curve-crossing in the 1.15 Å region between an energy surface initially rising to a C–H dissociation limit of several eV and a dissociative potential energy surface leading to the limit which experimentally is at 18.64 eV in Harland's study.⁶⁰ We can therefore rationalise the fact that our calculated (harmonic) frequency is ν₁(C–H) = 3347 cm⁻¹ for the C²Σ⁺ state whereas the frequency assigned by Baker and Turner⁴⁴ is 1320 cm⁻¹, by noting that our calculation is for the harmonic region of the potential energy surface close to the equilibrium structure region whereas the Franck-Condon vibrational overlap parameters creating the

He I photoelectron spectrum profile in the C²Σ⁺ state region mainly explore the shallow energy profile beyond the curve-crossing region.

We used a simple model to confirm this conjecture. Figure 7(c) shows that there are two minima in the C–H potential energy profile, one at r₁(C–H) = 1.0776 Å, which we associate with the calculated harmonic frequency ν₁(C–H) = 3347 cm⁻¹, and another at r₂(C–H) ≈ 1.37 Å. Using Badger's rule,^{110,111} that relates vibrational mode frequencies (bond force constants) in different electronic states of the same polyatomic molecule, we determined that at r₂(C–H) ≈ 1.37 Å the C–H potential energy profile corresponds to ν₁(C–H) ≈ 1465 cm⁻¹. Since this profile is very anharmonic, it is reasonable to expect the higher energy levels of the C²Σ⁺ state ν₁(C–H) mode to have further decreasing vibrational frequencies.

¹C. Moureu and J. C. Bongrand, *Ann. Chim.* **14**, 47 (1920).²M. A. Crowe and J. D. Sutherland, *ChemBiochem* **7**, 951 (2006).³M. Schwell, Y. Bénilan, N. Fray, M.-C. Gazeau, E. Ed-Sebbar, F. Gaie-Levrel, N. Champion, and S. Leach, *Mol. Phys.* **110**, 2843 (2012).⁴S. Leach, M. Schwell, G. Garcia, Y. Bénilan, N. Fray, M.-C. Gazeau, F. Gaie-Levrel, N. Champion, and J.-C. Guillemin, *J. Chem. Phys.* **139**, 184304 (2013).⁵B. E. Turner, *Astrophys. J.* **163**, L35 (1971).⁶T. Vasyunina, H. Linz, Th. Henning, I. Zinchenko, H. Beuther, and M. Voronkov, *Astron. Astrophys.* **527**, A88 (2011).⁷J. E. Lindberg, S. Aalto, F. Costagliola, J.-P. Pérez-Beaupuits, R. Monje, and S. Müller, *Astron. Astrophys.* **527**, A150 (2011).⁸L. Decin, M. Agúndez, M. J. Barlow, F. Daniel, J. Cernicharo *et al.*, *Nature (London)* **467**, 64 (2010).⁹D. Bockelée-Morvan, D. C. Lis, J. E. Wink, D. Despois, J. Crovisier *et al.*, *Astron. Astrophys.* **353**, 1101 (2000).¹⁰J. Crovisier, personal communication (2013).¹¹J. Crovisier, *Astron. Astrophys. Suppl. Ser.* **68**, 223 (1987).¹²G. L. Villanueva, K. Magee-Sauer, and M. J. Mumma, *J. Quant. Spectrosc. Radiat. Transfer* **129**, 158 (2013).¹³V. Kunde, A. C. Aikin, R. A. Hanel, D. E. Jennings, W. C. Maguire, and R. E. Samuelson, *Nature (London)* **292**, 686 (1981).¹⁴C. M. Anderson, R. E. Samuelson, G. L. Bjoraker, and R. K. Achterberg, *Icarus* **207**, 914 (2010).¹⁵E. H. Wilson and S. K. Atreya, *J. Geophys. Res.* **109**, E06002, doi:10.1029/2003JE002181 (2004).¹⁶V. A. Krasnapolsky, *Icarus* **201**, 226 (2009).¹⁷V. Vuitton, R. V. Yelle, and M. J. McEwan, *Icarus* **191**, 722 (2007).¹⁸Y. L. Yung, *Icarus* **72**, 468 (1987).¹⁹D. W. Clarke and J. P. Ferris, *Icarus* **115**, 119–125 (1995).²⁰J. Ferris, B. Tran, J. Joseph, V. Vuitton, R. Briggs, and M. Force, *Adv. Space Res.* **36**, 251 (2005).²¹D. W. Clarke and J. P. Ferris, *Origins Life Evol. Biospheres* **27**, 225 (1997).²²R. J. Cody, M. J. Dezvoni, and S. Glicker, *J. Chem. Phys.* **82**, 3100 (1985).²³J. B. Halpern, G. E. Miller, H. Okabe, and W. Nottingham, *J. Photochem. Photobiol. A* **42**, 63 (1988).

- ²⁴J. B. Halpern, L. Petway, R. Lu, W. M. Jackson, and V. R. McCrary, *J. Phys. Chem.* **94**, 1869 (1990).
- ²⁵K. Seki, M. He, R. Liu, and H. Okabe, *J. Phys. Chem.* **100**, 5349 (1996).
- ²⁶T. Titarchuk and J. B. Halpern, *Chem. Phys. Lett.* **323**, 305 (2000).
- ²⁷F. A. Miller and D. H. Lemmon, *Spectrochim. Acta, Part A* **23**, 1415 (1967).
- ²⁸T. A. Cool, J. Wuang, K. Nakajima, C. A. Taatjes, and A. McLroy, *Int. J. Mass Spectrom.* **247**, 18 (2005).
- ²⁹K. Kameta, N. Kouchi, M. Ukai, and Y. Hatano, *J. Electron. Spectrosc. Relat. Phenom.* **123**, 225 (2002).
- ³⁰J. Wang, B. Yang, T. A. Cool, N. Hansen, and T. Kasper, *Int. J. Mass Spectrom.* **269**, 210 (2008).
- ³¹L. Nahon, N. de Oliveira, G. Garcia, J.-F. Gil, B. Pilette, O. Marcouillé, B. Lagarde, and F. Polack, *J. Synchrotron Radiat.* **19**, 508 (2012).
- ³²B. Mercier, M. Compin, C. Prevost, G. Bellec, R. Thissen, O. Dutuit, and L. Nahon, *J. Vac. Sci. Technol., A* **18**, 2533 (2000).
- ³³G. A. Garcia, H. Soldi-Lose, and L. Nahon, *Rev. Sci. Instrum.* **80**, 023102 (2009).
- ³⁴J. C. Pouilly, J. P. Schermann, N. Nieuwjaer, F. Lecomte, G. Grégoire, C. Desfrancois, G. A. Garcia, L. Nahon, D. Nandi, L. Poisson, and M. Hochlaf, *Phys. Chem. Chem. Phys.* **12**, 3566 (2010).
- ³⁵M. Briant, L. Poisson, M. Hochlaf, P. de Pujo, M.-A. Gaveau, and B. Soep, *Phys. Rev. Lett.* **109**, 193401 (2012).
- ³⁶H.-J. Werner, P. J. Knowles, G. Knizia, F. R. Manby, M. Schütz *et al.*, MOLPRO, version 2012.1, a package of *ab initio* programs, 2012, see <http://www.molpro.net>.
- ³⁷K. Raghavachari, G. W. Trucks, J. A. Pople, and M. Head-Gordon, *Chem. Phys. Lett.* **157**, 479 (1989).
- ³⁸P. J. Knowles, C. Hampel, and H.-J. Werner, *J. Chem. Phys.* **99**, 5219 (1993); **112**, 3106 (2000) (Erratum).
- ³⁹C. Adamo and V. Barone, *J. Chem. Phys.* **110**, 6158 (1999).
- ⁴⁰P. J. Knowles and H.-J. Werner, *Chem. Phys. Lett.* **115**, 259 (1985).
- ⁴¹H.-J. Werner and P. J. Knowles, *J. Chem. Phys.* **82**, 5053 (1985).
- ⁴²P. J. Knowles and H.-J. Werner, *Chem. Phys. Lett.* **145**, 514 (1988).
- ⁴³T. H. Dunning, *J. Chem. Phys.* **90**, 1007 (1989).
- ⁴⁴C. Baker and D. W. Turner, *Proc. R. Soc. A* **308**, 19 (1968).
- ⁴⁵L. Åsbrink, W. Von Neissen, and G. Bieri, *J. Electron Spectrosc. Relat. Phenom.* **21**, 93 (1980).
- ⁴⁶A. A. Westenberg and E. B. Wilson, *J. Am. Chem. Soc.* **72**, 199 (1950).
- ⁴⁷J. K. Tyler and J. Sheridan, *Trans. Faraday Soc.* **59**, 2661 (1963).
- ⁴⁸J. K. G. Watson, A. Roytburg, and W. Ulrich, *J. Mol. Spectrosc.* **196**, 102 (1999).
- ⁴⁹(a) P. D. Mallinson and A. Fayt, *Mol. Phys.* **32**, 473 (1976); (b) P. D. Mallinson and R. L. de Zafra, *ibid.* **36**, 827 (1978).
- ⁵⁰L. A. V. Mendes, S. Boyé-Péronne, U. Jacovella, J. Liévin, and D. Gauyacq, *Mol. Phys.* **110**, 2829 (2012).
- ⁵¹P. Botschwina, M. Horn, S. Seeger, and J. Flügge, *Mol. Phys.* **78**, 191 (1993).
- ⁵²R. Kołos and J. C. Dobrowolski, *Chem. Phys. Lett.* **369**, 75 (2003).
- ⁵³J. B. P. Da Silva and M. N. Ramos, *Int. J. Quant. Chem.* **43**, 215 (1992).
- ⁵⁴M. Z. Kassae, S. Soleimani-Amiri, M. Majdi, and S. M. Musavi, *Struct. Chem.* **21**, 229 (2010).
- ⁵⁵S. Lee, *J. Phys. Chem.* **100**, 13959 (1996).
- ⁵⁶Y. Zhang, J. Guo, and J. Zhang, *Int. J. Mass Spectrom.* **309**, 56 (2012).
- ⁵⁷A. M. Smith-Glickhorn, M. Lorenz, R. Kołos, and V. E. Bondebey, *J. Chem. Phys.* **115**, 7534 (2001).
- ⁵⁸V. Cermak, and A. J. Yencha, *J. Electron. Spectrosc. Relat. Phenom.* **8**, 109 (1976).
- ⁵⁹J. Fulara, S. Leutweyler, J. P. Maier, and U. Spittel, *J. Phys. Chem.* **89**, 3190 (1985).
- ⁶⁰P. W. Harland, *Int. J. Mass Spectrom. Ion Proc.* **70**, 231 (1986).
- ⁶¹G. A. Garcia, L. Nahon, and I. Powis, *Rev. Sci. Instrum.* **75**, 4989 (2004).
- ⁶²J. Kreile, A. Schweig, and W. Thiel, *Chem. Phys. Lett.* **108**, 259 (1984).
- ⁶³M. Allan, E. Klosters-Jensen, and J. P. Maier, *Chem. Phys.* **17**, 11 (1976).
- ⁶⁴R. C. Gillen, B. Ostojic, and W. Domke, *Chem. Phys.* **272**, 1 (2001).
- ⁶⁵N. Komihya, P. Rosmus, and J. P. Maier, *Mol. Phys.* **104**, 3281 (2006).
- ⁶⁶T. A. Miller and V. E. Bondebey, *J. Chim. Phys.* **77**, 695 (1980).
- ⁶⁷J. C. Person and P. P. Nicole, *J. Chem. Phys.* **53**, 1767 (1970).
- ⁶⁸T. Ferradaz, Y. Bénilan, N. Fray, A. Jolly, M. Schwell, M. C. Gazeau, and H.-W. Jochims, *Planet. Space Sci.* **57**, 10 (2009).
- ⁶⁹H.-W. Jochims, H. Baumgärtel, and S. Leach, *Astron. Astrophys.* **314**, 1003 (1996).
- ⁷⁰J. Berkowitz, *Atomic and Molecular Photoabsorption* (Academic Press, New York, 2002), Chap. 3.
- ⁷¹Y. Hatano, *Phys. Rep.* **313**, 109 (1999).
- ⁷²V. H. Dibeler, R. M. Reese, and J. L. Franklin, *J. Am. Chem. Soc.* **83**, 1813 (1961).
- ⁷³U. Büchler and J. Vogt, *Org. Mass Spectrom.* **14**, 503 (1979).
- ⁷⁴G. Bieri, E. Heilbronner, V. Hornung, E. Kloster-Jensen, J. P. Maier, F. Thommen, and W. Von Neissen, *Chem. Phys.* **36**, 1 (1979).
- ⁷⁵B. Narayan, *Proc. Ind. Acad. Sci. A* **75**, 92 (1972).
- ⁷⁶J. L. Holmes, C. Aubry, and P. M. Mayer, *Assigning Structures to Ions in Mass Spectrometry* (CRC Press, Boca Raton, 2007).
- ⁷⁷S. G. Lias, J. E. Bartmess, J. F. Liebman, J. L. Holmes, R. D. Levin, and W. G. Mallard, *J. Phys. Chem. Ref. Data* **17**(Suppl. 1) (1988).
- ⁷⁸J. S. Knight, C. G. Freeman, M. J. McEwan, N. G. Adams, and D. Smith, *Int. J. Mass Spectrom. Ion Proc.* **67**, 317 (1985).
- ⁷⁹H. Okabe and V. H. Dibeler, *J. Chem. Phys.* **59**, 2430 (1973).
- ⁸⁰J. S. Francisco and S. L. Richardson, *J. Chem. Phys.* **101**, 7707 (1994).
- ⁸¹D. C. Parent, *J. Am. Chem. Soc.* **112**, 5966 (1990).
- ⁸²O. V. Dorofeeva and L. V. Gurvich, *Thermochim. Acta* **178**, 273 (1991).
- ⁸³J. W. Ochterski, G. A. Petersson, and K. B. Wiberg, *J. Am. Chem. Soc.* **117**, 11299 (1995).
- ⁸⁴S. Rayne and K. Forest, *Comp. Theor. Chem.* **970**, 15 (2011).
- ⁸⁵A. V. Golovin and V. V. Takhistov, *J. Mol. Struct.* **701**, 57 (2004).
- ⁸⁶See <http://webbook.nist.gov> for NIST Chemistry Webbook, National Institute of Standards and Technology Reference Database (2011).
- ⁸⁷J. Berkowitz, W. A. Chupka, and T. A. Walter, *J. Chem. Phys.* **50**, 1497 (1969).
- ⁸⁸K. P. Huber and G. Herzberg, *Molecular Spectra and Molecular Structure. IV. Constants of Diatomic Molecules* (Van Nostrand Reinhold, New York, 1979).
- ⁸⁹O. Kostko, J. Zhou, B. J. Sun, J. S. Lie, A. H. H. Chang, R. I. Kaiser, M. Ahmedo *et al.*, *Astrophys. J.* **717**, 674 (2010).
- ⁹⁰D. G. Clifton, General Motors Corporation Technical Report on Approximate Thermodynamic Functions for the CN⁺(g) and CN⁻(g) ions, December 1965.
- ⁹¹G. Fischer and I. G. Ross, *J. Phys. Chem. A* **107**, 10631 (2003).
- ⁹²D. W. Turrell, W. D. Jones, and A. Maki, *J. Chem. Phys.* **26**, 1544 (1957).
- ⁹³G. Herzberg, *Electronic Spectra of Polyatomic Molecules* (Van Nostrand Reinhold, New York, 1966).
- ⁹⁴M. W. Chase, Jr., *NIST-JANAF Thermochemical Tables*, *J. Phys. Chem. Ref. Data Monograph* 9 (1998).
- ⁹⁵W. Tsang, in *Energetics of Organic Free Radicals*, edited by J. A. Martinho Simoes, A. Greenberg, and J. F. Liebman (Blackie, London, 1996), pp. 22–58.
- ⁹⁶D. F. McMillen and D. M. Golden, *Annu. Rev. Phys. Chem.* **33**, 493 (1982).
- ⁹⁷K. Norwood and C. Y. Ng, *J. Chem. Phys.* **91**, 2898 (1989).
- ⁹⁸G. K. Jarvis, K.-M. Weitzel, M. Malow, T. Baer, Y. Song, and C. Y. Ng, *Phys. Chem. Chem. Phys.* **1**, 5259 (1999).
- ⁹⁹K.-C. Lau and C. Y. Ng, *J. Chem. Phys.* **122**, 224310 (2005).
- ¹⁰⁰J. Berkowitz, *Photoabsorption, Photoionization and Photoelectron Spectroscopy* (Academic Press, New York, 1979), p. 284.
- ¹⁰¹E. Lindholm, *Ark. Fys.* **40**, 97 (1968).
- ¹⁰²R. E. Connors, J. L. Roebber, and K. Weiss, *J. Chem. Phys.* **60**, 5011 (1974).
- ¹⁰³P. Botschwina, M. Horn, J. Flügge, and S. Sigrun, *J. Chem. Soc. Faraday Trans.* **89**, 2219 (1993).
- ¹⁰⁴X. Yang, S. Maeda, and K. Ohno, *Chem. Phys. Lett.* **418**, 208 (2006).
- ¹⁰⁵T. Wang, M. A. Buntine, and J. H. Bowie, *J. Phys. Chem. A* **113**, 12952 (2009).
- ¹⁰⁶P. W. Harland and R. G. A. R. Maclagan, *J. Chem. Soc., Faraday Trans. 2* **83**, 2133 (1987).
- ¹⁰⁷Y. H. Ding, X. R. Huang, Z. Y. Lu, and J. N. Feng, *Chem. Phys. Lett.* **284**, 325 (1998).
- ¹⁰⁸Y. H. Ding, X. R. Huang, Z. S. Li, and J. Y. Liu, *J. Mol. Struct.: THEOCHEM* **454**, 61 (1998).
- ¹⁰⁹S. Petrie, K. M. McGrath, C. G. Freeman, and M. J. McEwan, *J. Am. Chem. Soc.* **114**, 9130 (1992).
- ¹¹⁰R. M. Badger, *J. Chem. Phys.* **2**, 128 (1934).
- ¹¹¹R. M. Badger, *J. Chem. Phys.* **3**, 710 (1935).